Calibration of a high-volume gamma-ray scintillation spectrometer in the high-energy range

Kalibrace velkoobjemového scintilačního spektrometru gama záření v oblasti vyšších energií

David Kuča

Bachelor Thesis

Supervisor: Mgr. Radim Uhlář Ph.D.

Ostrava, 2022

VSB – Technical University of Ostrava
Faculty of Electrical Engineering and Computer Science
Department of Physics

Bachelor Thesis Assignment

Student: **David Kuča**

Study Programme: B0533A110023 Applied Physics

Title: Calibration of a high-volume gamma-ray scintillation spectrometer in the high-energy range
Kalibrace velkoobjemového scintilačního spektrometru gama záření v oblasti vyšších energií

The thesis language: English

Description:

1. Literature research: radioactivity, sources of ionizing radiation, detection of ionizing radiation, interaction of ionizing radiation with matter, principle of operation of D-T neutron generator, neutron activation analysis

2. Selection and preparation of standards containing appropriate elements for efficient calibration of large-volume NaI(Tl) spectrometer

3. Activation of standards by fast neutrons, energy and efficiency calibration of the spectrometer

References:

Gilmore, G.R. Practical Gamma-ray Spectrometry. John Wiley & Sons, 2008.

IAEA, Neutron generators for analytical purposes, Vienna 2012.

Interactive Chart of Nuclides. 2020 [online]. Available: https://www.nndc.bnl.gov/nudat2/ [Accessed Jan. 27th, 2020].

Knoll, G.F. Radiation Detection and Measurement. John Wiley & Sons, 2010.

Valković, V. 14 MeV Neutrons: Physics and Applications, CRC Press, Boca Raton, 2016.

Extent and terms of a thesis are specified in directions for its elaboration that are opened to the public on the web sites of the faculty.

Supervisor: **Mgr. Radim Uhlář, Ph.D.**

Date of issue: 01.09.2021

Date of submission: 30.04.2022

_____   _____

prof. Dr. RNDr. Jiří Luňáček   prof. Ing. Jan Platoš, Ph.D.
Head of Department   *Dean*

Abstract

The purpose of this thesis is to calibrate a high-volume gamma-ray scintillation spectrometer in energy levels higher than those of natural radionuclides and common calibration standards. It is achieved by a method called neutron activation analysis, that utilizes slow and 14 MeV neutrons to bombard elements of H, C, N and O. These activated elements then dexcite with emission of gamma-rays with energies up to 11 MeV. The calibration on common standards allows us to only calibrate in the energy range below 3 MeV. The energy calibration in this range does not apply in the higher energy range as the calibration shifts with great deviations. Total of 36 measurements were performed to gather data on which the calibration would be carried out.

Keywords

Fast Neutrons, Gamma Spectroscopy, Neutron Generator, Neutron Activation Analysis, Energy Calibration

Abstrakt

Cílem této práce je kalibrace velkoobjemového scintilačního spektrometru gama záření v oblasti energií vyšších, než vyzařují přirozené radionuklidy a běžné kalibrační etalony. Toho je dosáhnuto metodou zvaná "neutronová aktivační analýza", která využívá pomalých a 14 MeV neutronů k bombardování prvků H, C, N a O. Tyto aktivované prvky poté podléhají deexcitaci doprovázená emisí gama záření s energiemi až 11 MeV. Kalibrace na běžných etalonech nám umožňuje kalibrovat pouze v oblasti energií do 3 MeV. Energetická kalibrace v této oblasti přestává platit v oblasti vyšších energií, kde dochází k posunu kalibrace s velkými odchylkami. Dohromady bylo provedeno 36 měření, aby byla získána data, na kterých by bylo možné kalibraci provést.

Klíčová slova

Rychlé neutrony, Gama Spektrometrie, Neutronový Generátor, Neutronová Aktivační Analýza, Energetická Kalibrace

Acknowledgement

Contents

List of Abbreviations

NAA	Neutron Activation Analysis
RRD	Reaction Rate Density
ENDF	Evaluated Nuclear Data File
IAEA	International Atomic Energy Agency
PPE	Personal Protective Equipment
MCA	Multi-Channel Analyzer
PGNAA	Prompt Gamma Neutron Activation Analysis
DGNAA	Delayed Gamma Neutron Activation Analysis
FNAA	Fast Neutron Activation Analysis
PFNA	Pulsed Fast Neutron Analysis
PHA	Pulse Height Analysis
GPIO	General Purpose Input/Output
DF	Duty Factor
NG	Neutron Generator

List of Tables

List of Figures

Introduction

To successfully and flawlessly measure gamma-rays of higher energies an energy calibration in the higher energy range is required. These energies are assigned to correct channels in the spectrum. No radionuclides or common calibration standards exceed the gamma-energy level of 3 MeV. To get past this level, a method of neutron activation analysis has to be carried out. By utilizing a MP320 Neutron Generator supplied to our laboratory by a company Thermo Fisher Scientific, a bombardment of H, C, N and O elements is carried out and leads to their activation and subsequent deexcitation followed by emission of gamma-energies ranging from 2 MeV to almost 11 MeV. These energy levels are then used for the calibration of high-volume NaI(Tl) spectrometer produced by a company Scionix Holland, which stands out for its energy resolution and size.

Chapters 1, 2 and 3 thoroughly describe the principles of radioactivity and nuclear physics that form the basis of gamma-ray detection, operation of neutron generators and mainly the basis of neutron activation analysis. Chapter 1 begins with description of fundamental processes behind nuclear physics and Chapter 2 and 3 gradually build up the whole theory surrounding the methods and equipment used in this thesis.

Chapter 4 outlines the foundations of gamma spectrometry and describes how energy and efficiency calibration is performed. Chapter 5 then covers the topic of neutron generators and their operation and utilization. Chapter 6 is the final one of the literature research as it describes the neutron activation analysis that led to a collection of data required for the calibration of the NaI(Tl) spectrometer.

Chapter 7 summarizes the properties and configuration of equipment and components used in our measurements and their role in the overall apparatus. Chapter 8 then focuses on the calibration itself and depicts spectra that have been used for the calibration. Analysis of the spectra, problems that came with it and verification of the correctness of the final calibration are all treated in Chapter 8 as well.

1.   Radioactive Decay and Radiation Detectors

Unstable atomic nuclei lose energy by radiation. This radiation is spontaneous and statistically random. There is no way that we can predict time when the process happens, neither can we determine which specific nucleon undergoes the process. Radioactive decay can also be achieved by interaction of nuclei with other particles. This event results in a nuclear reaction that is accompanied by ionizing radiation.

1.1   Law of Radioactive Decay

We cannot determine which nucleon or at what time the nucleon decays, but we can calculate how many nuclei probably underwent the process. This fundamental law is described by a following relation [1]:

$$\frac{\mathrm{d}N}{\mathrm{d}t} = -\lambda N, \tag{1.1}$$

where dN is the rate of decay in the time interval of the length dt, N is the number of nuclei contained in an original sample. λ is called the decay constant and can be simply described as a probability per unit time of the decay of any nucleus. λ does not depend on any physical quantity such as temperature and pressure and is characteristic for every radionuclide. Its unit is s^{-1}. The solution of Eq 1.1 gives us an integral form [2]:

$$N(t) = N_0 e^{-\lambda t}, \tag{1.2}$$

where N_0 is the number of nuclei at the time t = 0. As we can see, the decrease of the number of not decayed nuclei is exponential. The exponential behavior is depicted in Fig 1.1 (data from Tipler [1]).
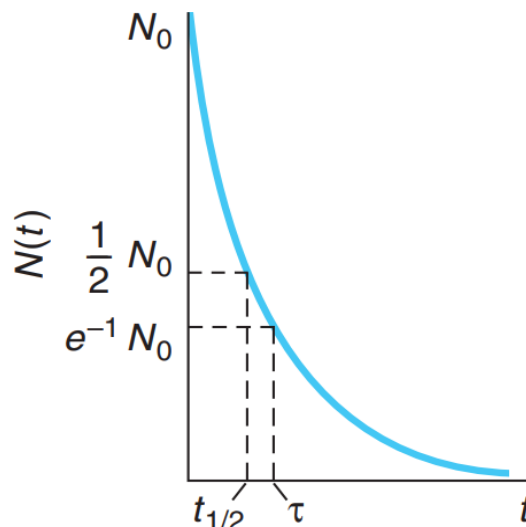
Figure 1.1: Exponential radioactive decay law.

For practical reasons we can transform the Eq. 1.1 by using a substitution:

$$A = -\frac{dN}{dt},$$
(1.3)

where A is called activity. It is described as a number of decays per time unit. The differential equation then changes to following equation:

$$A = \lambda N.$$
(1.4)

Solution of the Eq 1.3 gives us an integral form similar to Eq. 1.2 [2]:

$$A(t) = A_0 e^{-\lambda t}.$$
(1.5)

Another characteristic of every radionuclide is half-life $t_{1/2}$. Half-life is the time, in which half of the original nuclei decay. It is related to the decay constant λ described by the following relation [3]:

$$t_{1/2} = \frac{\ln(2)}{\lambda}.$$
(1.6)

Half-life times vary from microseconds to billions of years and the half-life values of all known radionuclides can be found in online databases, such as the IAEA databases [4].

Ways of energy lost due to radioactive decay can be categorized into three main types of radiation. If the energy is carried out in a form of emitted particles, we talk about alpha decay or beta decay. On the other hand, if the energy is transferred by an electromagnetic ray, it is called gamma rays or gamma radiation. Apart from this main difference, other characteristics such as range, mass, etc. are also typical for each form of decay. Let's take a look at them [2].

1.1.1 Alpha decay

Probably the most common type of radiation is alpha decay. Heavy nuclei are energetically unstable and tend to emit alpha particles, which can be considered as nuclei of helium $_2^4$He. By emitting alpha particle, the original nucleus decays into different, more stable nucleus with atomic number reduced by 2 and mass number reduced by 4 as shown in following scheme [1]:

$$_Z^A X \rightarrow _{Z-2}^{A-4} Y + _2^4 He.$$
(1.7)

Emitted alpha particles are monoenergetic and their energy is given by the law of conservation of energy and momentum and its value is between 4 and 6 MeV. The distance the alpha particles can fly in material is very short. By interacting with other particles in the air, the alpha particle loses energy until it has none. Due to this energy conversion, alpha decay cannot penetrate skin, can be shielded by a sheet of paper or simply by a short distance in the air. Even though its range is quite limited, alpha decay is still highly ionizing. This is caused by its charge of +2e which makes alpha particles have a high rate of energy loss when interacting with matter [5].

For instance, alpha radiation is typical for the decay of radium [6]:

$$_{88}^{226}Ra \rightarrow _{86}^{222}Rn + \alpha.$$
(1.8)

1.1.2   Beta decay

Just like alpha decay, beta radiation is made up of particles, more precisely charged particles. We split the description of beta radiation into two forms depending on the charge of particles – β⁺ and β⁻, sometimes referred to as positrons and negatrons. When the charge is positive, we consider beta decay as a ray of positrons, and we call it β⁺ radiation. Analogically, if the charge is negative, we call it β⁻ radiation and it is looked at like a ray of electrons. In comparison with alpha decay, beta particles are way faster because of their lower mass [2]. The decay can also be schematised, so for β⁻ decay the following scheme shows us that the atomic number of the original nucleus is increased by 1 and is followed by emission of antineutrino [3]:

$$_Z^A\text{X} \rightarrow\ _{Z+1}^{A}\text{Y} + \beta^- + \bar{\nu}, \tag{1.9}$$

whereas for β⁺ decay the atomic number is decreased by 1 and followed by emission of electron neutrino:

$$_Z^A\text{X} \rightarrow\ _{Z-1}^{A}\text{Y} + \beta^+ + \nu. \tag{1.10}$$

β⁻ decay is typical for a nucleus with an excess of neutrons, which undergo a conversion into protons as shown in following scheme [2]:

$$n\ \rightarrow p +\ e^- +\ \bar{\nu}. \tag{1.11}$$

If the nucleus has an excess of protons, then the β⁺ decay can be also observed on the conversion of protons into neutrons, which can be written as [5]:

$$p\ \rightarrow n +\ e^+ +\ \nu. \tag{1.12}$$

Their range is not much higher than the range of alpha particles, they can be shielded by a 1 meter width of air space or aluminum foil, so the possibility of beta decay penetrating human skin is fairly low, but it is still not safe to be exposed to beta decay for a long time. Energy of beta particles is a little bit lower than alpha particles, but unlike alpha particles, which are monoenergetic, beta particles come in a continuous spectrum of energies that can be described by *beta decay schemes* [5].

Internal Conversion

This difference is good to mention because of the fact that it is possible to capture and observe electrons emitted from the nucleus that are monoenergetic, so their origin can't be found in beta decay, but in a process called *internal conversion*. It is a form of gamma decay, but different in its principle. Usually, a nucleus in its excited state deexcites and emits a photon, but not in this case. Instead of emitting a photon, the nucleus emits one of its orbital electrons from the whole atom [2].

Electron Capture

Also similar to beta decay is an event called *electron capture*. A proton inside a nucleus captures an electron and changes into a neutron followed by the emission of a neutrino. This process is similar to β⁺ decay, because the atomic number of the original nucleus is also reduced by 1. Electron capture happens when the mass of an atom with atomic number Z is higher than of an atom with

atomic number Z − 1. The outcome of electron capture is usually an emission of characteristic X-rays or an emission of Auger electrons. Auger electrons are emitted when an electron from higher energy level fills a vacancy in lower energy level caused by the electron capture. The nucleus that was created from the electron capture is commonly in excited state, so gamma radiation occurs to get the nucleus to its ground state [1]. A typical example of electron capture is [2]:

$$^{40}_{19}\text{K} + e^- \rightarrow\ ^{40}_{18}\text{K} + \nu, \tag{1.13}$$

that is used for rock age determination.

1.1.3 Gamma Decay

Gamma decay differs from alpha and beta decay in its principle. Whereas during alpha and beta decay are emitted particles with non-zero rest mass particles (electrons or positrons), during gamma decay are emitted photons. They have no rest mass and no charge. Nucleus in an excited state emits energy in the form of a photon to get to a lower, more stable state of the same isotope. Gamma radiation is usually a by-product of beta decay. If we take a nucleus and let it decay, the beta radiation brings the nucleus to an excited state. Now we have an excited state of a nucleus which tends to become stable, so it emits gamma rays and gets to its ground state [3]. Photons are monoenergetic and their energy is equal to the difference between excited and final state, and its value is usually of the order of MeV.

Precise calculation is quite simple, and the result can be achieved by following equation [1]:

$$hf = E_{high} - E_{low}, \tag{1.14}$$

where h is called Planck constant with its value set at $4{,}13667696 \times 10^{-15}$ eV·Hz^{-1} and f is a frequency of the photon [1]. Nucleus deexcitation can be schematized as well [2]:

$$^{A}_{Z}\text{X} * \rightarrow\ ^{A}_{Z}\text{Y}(*) + \gamma. \tag{1.15}$$

The asterisk (*) means that the nucleus is in its excited state. The meaning of the asterisk being in brackets on the right side of the scheme is that the nucleus can decay to its lower, but still excited state instead of getting directly to the ground state. We can also notice that no changes happen to A or Z, that's because the decay is associated with a change in energy states, no particles are emitted from the nucleus [2].

Exposure to gamma radiation can cause severe health problems due to its penetration ability. When gamma rays interact with matter, it does not lose energy so rapidly like alpha or beta decay and can penetrate more deeply into a human body. Interaction with matter is followed by a high ionization of the material, but this ionization is still lower than of alpha decay, however, it doesn't make it less hazardous, but vice versa the inability to efficiently shield the radiation makes it more difficult to deal with. Gamma radiation can be shielded by a thick wall of concrete, but its width must be approximately 1 meter, or thinner layer of lead. Besides its penetration ability, an even bigger danger is the direct and immediate damage to cells on impact, increased exposure can also cause cancer [8].

1.2 Sources of Ionizing Radiation

In previous subchapters we've roughly described principles and physical nature of each type of radiation so now we should ask the question "where does the radiation actually come from?". People habitually think of a radioactive material as some kind of glowing metal stick, but this is a misconception. Generally known sources of radiation are radioactive materials, dominantly metals called *actinide*, that are found in natural resources, but they certainly do not glow on their own. These metals are also not the only source, radiation can also come from space, and we refer to this radiation as *cosmic radiation*. Simply said, cosmic rays are a form of high energy radiation that comes from outside of the solar system [9].

Sources don't need to be natural. Since the discovery of radioactivity, besides the science advancement in observing radioactivity, scientists have also made progress in creation of man made sources of radiation. From isotopes made in a laboratory, to whole machines capable of emitting any type of radiation, scientists are able to create a source, control it and also shut it down [9]. To make it less diverse and so we can focus better on each source of radiation, let's describe all possible sources of radiation for each type of decay.

1.2.1 Sources of alpha particles

Alpha particles are mainly emitted from unstable atoms with a low neutron to proton ratio. Such a characteristic is mainly observed with elements from the actinide series such as thorium, americium, etc. Typical alpha emitters that are not from actinide series are isotopes of radium, radon, that are decay products of probably the most known alpha particle emitter – uranium [9]. Series of cascading radioactive decays from a prime nuclide, referred to as *parent nuclide,* to decay products called *daughter nuclide*, that undergo another decay, are called *decay chains*. Its scheme shows us how a radioactive nucleon decays to the most stable decay product, where the decay chain stops [10]. An example of decay chain of ^{238}U is depicted in Fig. 1.2 [11].
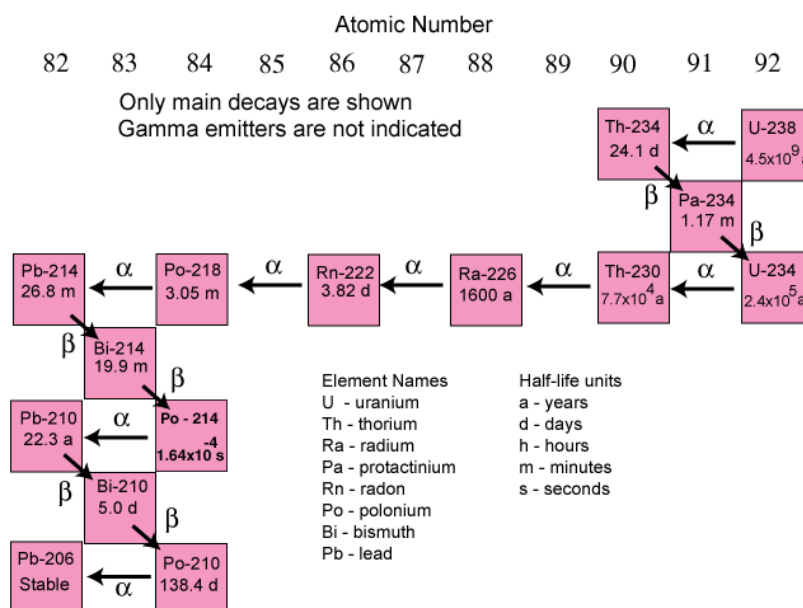
Figure 1.2: The decay scheme of ^{238}U.

Less significant sources of alpha particles are energetic helium nuclei, conventionally referred to as alpha particles, that are produced by scientists in particle accelerators. High-energy helium nuclei also make up 10 – 12% of cosmic radiation. Alpha particles created by *ternary fission*, which is a type of nuclear fission in that three charged alpha particles are created instead of two, have also three times more energy than common alpha particles, thus their range is a bit higher [12].

1.2.2 Sources of beta particles

The origin of beta particles is pretty much the same as of alpha particles – they also come as a result of radioactive nuclide decays. However, things are different for β^- and β^+ particles. Electrons are emitted from unstable nuclei with a high neutron to proton ratio, unlike positrons, where the ratio is low. As we mentioned earlier, beta decay also comes up from the conversion of proton to neutron, or reversely [9]. Some pure sources of β^- and particles are listed in Table 1.1 (data from Gilmore [6]).

Nuclide	Half-life	Maximum beta energy (keV)
^{3}H	13,312 yrs	19
^{14}C	5700 yrs	156
^{32}P	14,284 d	1711
^{35}S	87,32 d	167
^{36}Cl	$3,01 \times 10^5$ yrs	1142
^{45}Ca	162,6 d	257
^{63}Ni	98,7 yrs	66
^{90}Sr	28,8 yrs	546
^{90}Y	2,6684 d	2282
^{99}Tc	$2,111 \times 10^5$ yrs	294
^{147}Pm	2,6234 yrs	225
^{204}Tl	3,788 yrs	763

Table 1.1: Characteristics of some beta- emitters.

1.2.3 Sources of gamma radiation

Alpha and beta decay is closely related to gamma radiation. Beta decay leads to a higher population of excited states of nuclei, resulting in deexcitation of these nuclei and an emission of gamma radiation. Briefly we can say that the predominant source of gamma radiation is radioactive excited nuclide. Another source of high-energy photons is manmade and is known as *X-ray* [3]. We are not going to mention X-ray further in this work, so the precise description of its principle is not needed.

2.   Neutrons

A proton was discovered by Rutherford in the early 1900s, but he's been met with several difficulties in explaining why the atomic number was always less than the atomic mass. He came to the conclusion that the difference must be caused by another particle in the nucleus. Few years later, Bothe and Becker published remarkable results of some of their experiments, in which they observed an interaction between alpha radiation and elements like lithium, or boron. A new form of radiation emitted from this reaction was more penetrating than gamma radiation, but they didn't exactly know where this radiation came from. Little bit later in time, British scientist James Chadwick has taken this hint and has carried out several experiments to support his theory about the existence of chargeless particles. In 1932, he published an article about the existence of the particle being „theoretically possible", followed with a definitive announcement published 3 months later saying that the particles actually do exist and called them neutrons. Along with experimental results, technical information about neutrons were provided as well. This discovery led to James Chadwick being awarded the Nobel Prize in 1935 and a chain of new discoveries has begun [13].

2.1   Characteristic of Neutrons

As we know from the previous paragraph, protons in the nucleus are accompanied by other particles – neutrons. Collectively they are called nucleons and they both share similar properties. Its mass is about the same as that of protons, precisely $1,67492728 \times 10^{-27}$ kg (NIST 2018 [14]), that means the neutron is 1,001378 times heavier than proton. The mass difference could be explained by a more detailed description of the nucleon composition. Both neutron and proton, categorized as hadrons, are composed of three quarks, neutron (udd) is composed of one up quark (u) and two down quarks (d), whereas proton (uud) is composed of two up quarks and one down quark [13]. We consider a neutron as a fermion too, because it has a spin of ½. A deuteron, which is an atom made of one proton and one neutron, is formed. The mass of neutron can be calculated from the binding energy of the deuteron [15]:

$$m_{\mathrm{d}} = m_{\mathrm{p}} + m_{\mathrm{n}} - \frac{E_{\mathrm{d}}}{c^2}. \tag{2.1}$$

A deuteron has a spin 1 and a orbital angular moment 0, thus the neutron has to have a spin of 1/2 or 3/2, since a proton has a spin 1/2. The spin 3/2 can be certainly excluded due to various experiments [15]. Just like protons, neutrons can exist outside of a nucleus on their own. But its half-life of 10,2 minutes makes it rare to find on its own, because a free neutron undergoes a conversion to proton followed by emission of antineutrino and β^- particle (e⁻) as shown in the Eq. 1.11 [13].

Unlike protons, neutrons carry no charge; that's also where the name „neutron" comes from – it is neutral. Since it is uncharged, there is no Coulomb repulsion preventing it from interacting directly with a nucleus and making neutrons capable of deeper penetration than any other type of radiation. Its interaction with matter does not result in ionization, but it may cause nuclear reactions. Such a reaction then creates other types of radiation that we have talked about. This fact will be key

for following chapters. Another important characteristic of neutrons is its magnetic moment with the value set at -9,6623651 x 10^{-27} J.T^{-1} [14-15]. Characteristics of a neutron compared to other light particles are listed in Table 2.1 (data from [15]).

Particle	Mass (g)	Mass in Atomic Weight Units *u*	Charge	Spin
Neutron	1,674666×10^{-24}	1,008665	<10^{-18} e	½
Proton	1,672357×10^{-24}	1,007276	e	½
H-Atom	1,673268×10^{-24}	1,007825	-	-
Deuteron	3,343057×10^{-24}	2,013554	e	1
Electron	9,1081×10^{-28}	5,4859×10^{-4}	-e	½

Table 2.1: Comparison of properties of neutron to other light particles.
Atomic Weight Unit u = 1,660277×10^{-24} g (=1/12 of the mass of C-12 atom).

There is a high variety of reactions coming up from interactions of neutrons with nuclei, so to narrow it down, we should classify neutrons into groups according to their kinetic energies. There are three main groups. **Slow neutrons** are those with energies lower than 1000 eV. **Intermediate energy neutrons** have their energies in the range of 1 keV < E < 500 keV. Last group of neutrons is called **fast neutrons** and they have energy E > 500 keV [15].

Another common terminology, that is expanding the description of slow neutrons, is a kind of thermodynamic simile as shown in Table 2.2 (data from [16]):

Term	Energy	Velocity (m/s)	Temperature (K)
ultra cold	<0,2 μeV	<6	<0,002
very cold	0,2 μeV < E < 50 μeV	6 < *v* < 100	0,002 < *T* < 0,6
cold	0,05 meV < E < 25 meV	100 < *v* < 2200	0,6 < *T* < 300
thermal	25 meV	2200	300
epithermal	25 meV < E < 500 keV	2200 < *v* < 10^7	
fast	>500 keV	>10^7	

Table 2.2: Terminology of neutron energies.

2.2 Neutron sources

One can say that there are no natural sources of neutrons based on the fact that neutrons' half-life is very short. Although there's a little bit of truth to it when we talk about spontaneous fission of transuranic heavy nuclides, we could say that neutrons are made artificially. Neutron emission from excited nuclei decay is observable, but it's not a result of any natural spontaneous decay process. Neutrons are predominantly created as a result of nuclear reaction or in neutron generators [3]. For a neutron to be freed from nuclei in nuclear reaction, target material is bombarded by alpha particles, protons, deuterons or gamma rays. The most important condition must be met to make a neutron emission possible – nuclei excited from the bombardment must have its excitation energy larger than

the binding energy of neutrons in nuclei. The remaining energy is then split between the residual nucleus and created neutrons as their kinetic energy. [15]

(α, n) Reactions

Alpha particles are a product of decay of radionuclides, so a fabrication of a small neutron source can be done by combining a suitable target material with a convenient alpha emitter [3]. In a reaction [15]:

$$_Z^A\text{X} + {}_2^4\text{He} \rightarrow {}_{Z+2}^{A+3}\text{Y} + n + Q, \tag{2.3}$$

Q signifies the energy released or absorbed in the reaction. If Q is higher than 0, the reaction is exothermic, if Q is lower than 0, the reaction is endothermic. The maximum neutron yield is achieved when beryllium is bombarded with alpha particles, then the Q-value is +5,704 MeV [15]:

$$_4^9\text{Be} + {}_2^4\text{He} \rightarrow {}_6^{12}\text{C} + n + 5,704 \text{ MeV}. \tag{2.4}$$

But because of the weak penetration ability of alpha particles, most of them are stopped by the material and only 1 in 10000 reacts with the beryllium nucleus. A formation of combined source of alpha emitter and target material is realizable. Optimal alpha emitters are actinide elements and a formation of alloy between actinide metals and beryllium create a combined source. There are several alloys that improve neutron yield of beryllium that usually consist of Pu, Po, Am or Cm. There are also alternative isotopic neutron sources, the most important are listed in Table 2.3 (data from [3]). We must consider the cost, availability and half-life of these alloys and alternative sources as well, because not all of actinide metals are cheap to obtain, or suitable for needs. [3]

Target Material	Reaction	Q-value (MeV)	Neutron Yield per 10^6 Alpha Particles
Natural B	^{10}Be(α,n)	+1,07	13 for ^{241}Am alpha particles
	^{11}B(α,n)	+0,158	
F	^{19}F(α,n)	-1,93	4,1 for ^{241}Am alpha particles
Isotopically separated ^{13}C	^{13}C(α,n)	+2,2	11 for ^{238}Pu alpha particles
Natural Li	^{7}Li(α,n)	-2,79	
Be for comparison	^{9}Be(α,n)	+5,71	70 for ^{241}Am alpha particles

Table 2.3: Alternative isotopic neutron sources and comparison to Be target.

(d, n) Reactions and Accelerated Charged Particles Reaction

The bombardment with deuterons or protons leads to a production of highly excited nucleus and neutrons. Usually, protons and deuterons must be artificially accelerated in laboratories to obtain sufficient energy for making the reactions possible. Most of these reactions are exothermic. We are going to devote more time to two special reactions [3]:

$$_1^3\text{H} + {}_1^2\text{H} \rightarrow {}_2^4\text{He} + n + 17,6588 \text{ MeV}, \tag{2.5}$$

$$_1^2\text{H} + {}_1^2\text{H} \rightarrow {}_2^3\text{He} + n + 3,26 \text{ MeV}, \tag{2.6}$$
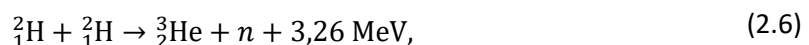
which are fundamental reactions in D-T and D-D neutron generators (see Section 5.2) [3].

(γ, n) Reactions

When a target nucleus is supplied with enough excitation energy by absorbing a gamma ray photon, a free neutron is emitted. To make emission possible, the photon has to have an energy of at least the negative of the *Q*-value, so high-energy gamma rays are required in order to produce neutron sources for observation purposes. This fact is also important for choosing target nuclei, since gamma-rays rarely exceed the energy of 3 MeV, only two, ^{9}Be and ^{2}H, are suitable and significant for practical uses [15]:

$$^9_4\text{Be} + \gamma \rightarrow {}^8_4\text{Be} + n - 1{,}666 \text{ MeV}, \tag{2.7}$$

$$^2_1\text{H} + \gamma \rightarrow {}^1_1\text{H} + n - 2{,}226 \text{ MeV}. \tag{2.8}$$
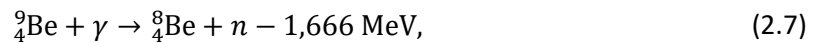
The formation of photoneutron sources is also possible, also among this advantage there is another important aspect of photoneutrons – since photons are monoenergetic, photoneutrons are monoenergetic as well [3]. On the other hand, working with larger photoneutrons sources requires better protection against the penetration of gamma-rays.

Spontaneous Fission

There is a chance that heavy atomic nuclei can decay by spontaneous fission, but it is relatively rare. Not all, but few of those nuclei can decay by emission of fast neutrons, so we can consider heavy nuclei as a source of neutrons [15]. In addition to the emission of neutrons, other types of radiation are produced in reactions that have to be shielded by an appropriate material of the container where the neutron source is stored. From the transuranic group, which is known to be mostly alpha-emitters, Cf-252 and Pu-240 are the most widely used sources. The half-life of Cf-252 is 2,65 years, thus it is convenient for this use, and from a microgram of material $2{,}30 \times 10^6$ n/s is produced [3].

3.   Interaction of Radiation with Matter

Understanding the principles behind interaction of neutrons or ionizing radiation with matter clears the path to better knowledge of how radiation detectors work, how we should protect ourselves from radiation, and especially how we can use these interactions in analysis that concerns this work further in the text. The fundamental principle behind interaction with matter is the loss or conversion of energy between matter particles and incident particles/rays. Since we know that charged particles interact through the Coulomb force, whereas photons do not carry any charge, thus Coulomb force doesn't concern them, it is better for us to divide interactions based on what type of particle/rays interacts with matter [3].

3.1   Interaction of Each Ionizing Radiation Type

Unlike neutrons, ionizing radiation directly ionizes matter on impact, therefore these interactions are different and it's better to discuss each type of ionizing radiation separately.

3.1.1   Interaction of Alpha Particles with Matter

Heavy charged particles interact preferably through Coulomb forces with other oppositely charged particles, in this case negatively charged orbital electrons of the matter's atom. Since the possibility of alpha particles interacting with nuclei is significantly lower, thus it is not important for our further description [3]. When a heavy charged particle enters the matter, it simultaneously exerts a force on multiple electrons in orbitals of atoms in the vicinity of the particle and transfers its energy in *inelastic collision* [18]. Electrons are then raised to a higher level of the shell within the atom, resulting in excitation, or it is completely removed from the atom and continues on its own, resulting in ionization and a production of ion pairs. Ion pair consists of an electron removed from the atom's shell and its opposite ion, together they then tend to form a neutral atom. Since the energy of the alpha particle is partly transferred to the electron, its velocity decreases. It may seem that only a small fraction of an alpha particle's energy is lost due to the interaction, but the particle reacts with many electrons at the same instant, so it loses energy on a larger scale and is eventually stopped completely [3]. Its range is the shortest of any type of radiation due to its large mass and positive charge of +2, making it lose energy rapidly in the matter [19].

3.1.2   Interaction of Beta Particles With Matter

Upon entering a material, electrons and positrons lose energy at a lower rate than heavy particles due to their lower mass and different charge (±e). In comparison with alpha particles, electrons can lose more energy in single interaction with electrons in the valence level of the atoms shell. Charged particles act on the matter through electromagnetic force. When an electron encounters another electron of matter's atom, ionization occurs when the orbiting electron is displaced, or the atom is excited. Colliding electron loses its kinetic energy and is slowed down and eventually, when the electron is slow enough, it is captured by the atom of the material and also the

Bremsstrahlung can occur [19]. Since the mass of a traveling electron is the same as the mass of electrons within a material's atom, it's path and direction is changed way easily causing bigger deviations in its movement within the matter. The particle can be swerved by the elastic scattering with the nucleus as well [20]. On the other hand, when positrons interact with electrons within the atom's shell, they are annihilated and the reaction produces two photons both with energy of 0,511 MeV. The range of electrons and positrons is longer than for alpha particles, but still short. Beta radiation can be stopped by a few centimeters of any metal [19]. The absorption of beta particles is exponential and can be described by following relation [3]:

$$I = I_0 e^{-\mu t},$$ (3.1)

where I_0 is a counting rate without absorber, I is counting rate with observer, t is the thickness of absorber and μ is absorption constant. The Figure 3.1 [3] represents the transmission plot of monoenergetic electrons given by the by extrapolation of the linear portion of the curve to zero, where R_e is extrapolated range [3].
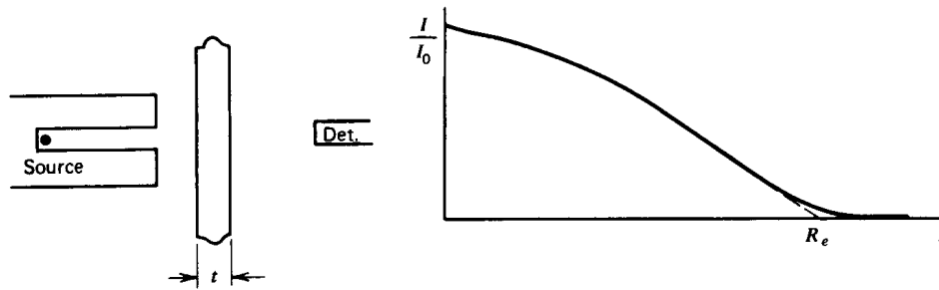
Figure 3.1: The transmission curve for monoenergetic electrons.

3.1.3   Interaction of Gamma Rays With Matter

First of all, gamma radiation energy is not carried by particles, but by photons forming electromagnetic rays. Photon has no rest mass, nor a charge, so the penetration ability is weaker and materials of better properties are required in order to stop it completely [19]. There are three main methods of describing how gamma rays interact with matter, fairly depending on the energy of the radiation. All of them result in the total or partial transfer of energy to electrons.

Photoelectric absorption is dominant at low energy of a photon. When gamma-ray photon interacts with one electron within the atom, the electron is then ejected from the shell and continues with a kinetic energy E_e given by [6]:

$$E_e = E_\gamma - E_b,$$ (3.2)

where E_γ is the energy of the interacting photon and E_b is the binding energy of the electron in its shell. For energies lower than a few hundreds of keV the photon is considered to fully disappear and transfer all of its energy to electron. Affected atom is then left in an excited state, therefore it tends to dexcite to achieve an equilibrium. This can result in an emission of Auger electrons [6]. As another option, the ejection of an electron (mostly K electron) creates a vacancy within the shell. If the vacancy is filled by

capturing a free electron or electrons in other levels of the shell are rearranged, then characteristic X-ray photons are arised. There is a slight chance that X-ray escapes the detector and causes deviations in measurements known as *escape peaks* [3]. The Figure 3.2 depicts the principle of photoelectric absorption [6]:
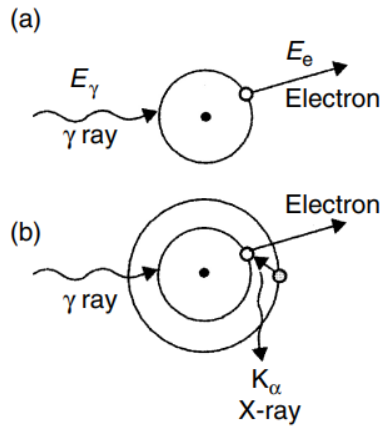
Figure 3.2: (a) The mechanism of photoelectric absorption; (b) the emission of X-rays.

Compton scattering is the most often occuring interaction between gamma-ray photon and electron, but in this case only a portion of photon's energy is transferred to electron. The path of the gamma-ray is diverted by impact and its energy is decreased by transferring a part of the energy to electron. How much the energy of gamma-ray is changed can be shown in following equation [6]:

$$E_e = E_\gamma \left\{ 1 - \frac{1}{[1 + E_\gamma(1 - cos\theta/m_0 c^2]} \right\}. \tag{3.3}$$

We can notice that the energy absorbed varies with the angle θ of the scattering, in more detail, at small angles θ very little energy is transferred as shown in Figure 3.3 [6]. For elements with higher Z the probability increases linearly, because the number of electrons available for the scattering increases [3].
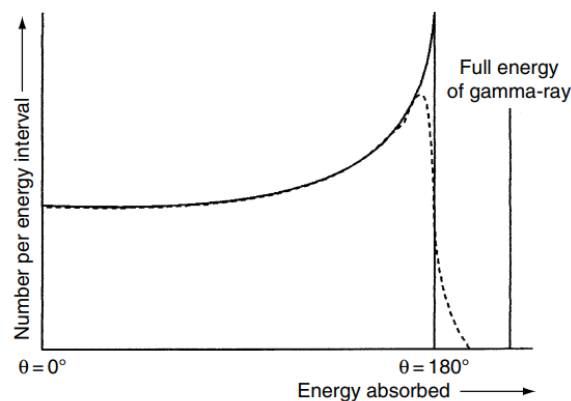
Figure 3.3: Energy transferred to absorber related to scattering angle.

23

Pair production is an interaction possible only after one crucial condition is met – the energy of incident gamma-ray must be at least equivalent to the combined rest mass of the electron and positron which is 1,022 MeV. Therefore pair production is typical for gamma-ray photons with higher energies [6]. The interaction takes place within the Coulomb field of the nucleus and the gamma-ray photon interacts with the atom as whole. In the process the gamma-ray disappears and a pair of electron-positron is created. Since positron is then slowed down in the matter and annihilates, two annihilation photons are produced both with an energy of 511 keV [3]. The whole process is described in Figure 3.4 [6]:
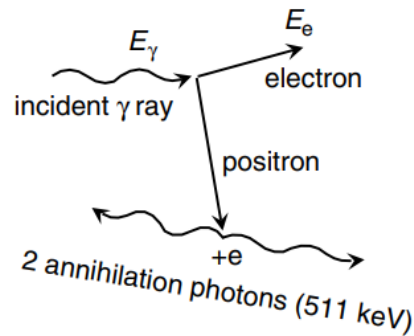
Figure 3.4: The mechanism of pair production and annihilation of positron.

3.2   Interaction of Neutrons With Matter

The most substantial topic for our research is the interaction between neutrons and target material. Reactions concerning Neutron Activation Analysis (NAA) are going to be discussed later, because its principles are more complex and we should take more space to describe them in more depth. This section is a brief summary of interactions with matter and we will also describe what *cross section* means.

3.2.1   Interactions

There are several interactions that could happen when a neutron encounters a nucleus. Some of them only happen under exact circumstances, and the probability of each interaction correlates with neutron energy. Since neutrons are chargeless, they are not subject to Coulomb forces and therefore they are able to penetrate the matter without undergoing any interaction within a few centimeters in the matter. Two major types of interaction divide the whole subject of interactions into two groups – scattering and absorption. After an interaction, a neutron can either totally disappear, be replaced by secondary radiation, or its direction or energy is changed remarkably [3]. Secondary radiation is usually described by a simple notation giving us a clear depiction of what is the product of the reaction. If a neutron n impacts a target material T and particle g is arised forming a nucleus R as a result of the reaction, then the reaction is simply written as T(n,g)R [21].

Most important interactions are:

- **Elastic scattering** occurs when the neutron encounters the nucleus. This reaction is typical for slow neutrons, which have a small amount of energy, so the energy can't be completely transferred to the nucleus. The result of the interaction is a decrease in kinetic energy and different direction of the neutron movement [17]. The cascade reduction of a neutron's kinetic energy is a fundamental mechanism in *neutron thermalization*. Each collisions slows down the slow neutron into a thermal equilibrium and the process of average energy loss can be described by following relation:

$$E_n = \frac{2E_0 A}{(A+1)^2} \tag{3.4}$$

  where E_0 is the energy of the incident neutron and *A* is atomic weight of the nucleus. For example, if a slow neutron with an energy of 2 MeV collides with a nucleus of hydrogen with A = 1, therefore its energy reduces to 1 MeV. After a total of 27 collisions the neutron reaches an energy of 0,025 eV, which is considered as an energy of a *thermal neutron.* Also, hydrogen has almost the same mass as neutron, so H is the most efficient neutron moderator [21].

- **Inelastic scattering** comes about when we use fast neutrons for interactions, because their energy must be above the energy of the first excited state of the affected nucleus. This case differs from elastic scattering, because the kinetic energy of a neutron is partially transferred to the nucleus in order to put it in its excited state [21]. The affected nucleus then quickly de-excites resulting in emission of gamma radiation and the neutron continues with lower energy and in a different direction. It is possible to use previously mentioned symbols for this reaction – (n,n') or (n,n'γ). The secondary radiation complicates the question of shielding when using fast neutrons due to the penetration ability of both neutrons and gamma radiation [3].

- **Neutron Capture** or (n,γ) reaction is the most efficient for capture of slow neutrons, but in this case, instead of the neutrons being scattered by the nucleus, they are absorbed or captured. Compound nucleus is formed and a rearrangement of its structure follows. In about 10^{-10} seconds, the excited nucleus decays and one or more gamma-rays are released from the nucleus [21]. For example, when a stable ^{59}Co absorbs a neutron radioactive isotope ^{60}Co forms and immediately decays by an emission of beta particle and then gamma-rays. In fact, neutron capture is a dominant process responsible for formation of transuranic elements [13]. The process of neutron capture is a fundamental principle for the **Neutron Activation Analysis**, which we will discuss later (see Section 6.1).

- **Charged particle emission** is a byproduct of neutron capture. Besides the emission of gamma-rays, other charged particles can be produced as well, commonly protons, deuterons and alpha particles, shortly (n,p),(n,d) and (n,α) reactions [13]. Some of these reactions are more likely than (n,γ) reaction and two of the most significant (n,α) reactions for practical use in neutron detection and shielding are ^{6}Li(n,α)^{3}H and ^{10}B(n,α)^{7}Li*. In the second case, the product of reaction is ^{7}Li, which is in excited state, so an emission of gamma-rays follows, therefore the

whole process can be symbolized as ^{10}B(n,αγ)^{7}Li. Likewise, the reaction ^{3}He(n,p)^{3}H also plays an important role in neutron detection [17].

- **Nuclear Fission** or (n,f) is an interaction between a neutron and heavy nucleus, sometimes described as fissionable nucleus. Upon capture of the neutron by a heavy nucleus, the nucleus splits into two fragments, both of a mass about one half of the original nucleus, together with emission of another one or two fast neutrons. This process is widely used in nuclear energy production where ^{235}U or ^{239}Pu is used for bombardment by neutrons eventuating in chain reaction producing a high amount of energy [13].

- **Reactions (n,2n) and (n,3n)** are neutron capture reactions that occur when using fast neutrons (especially 14 MeV neutrons produced by a neutron generator) that have enough energy to overcome a threshold energy, leading to a reaction that produces more neutrons occurs [13].

3.2.2   Cross Section

If we consider a huge amount of neutrons targeting a material, some of them may either penetrate the material without undergoing any interaction or some can interact with the nucleus. For neutrons of a fixed energy, the probability of interaction per unit path length is constant and is expressed in terms of the *cross section σ* per nucleus for each type of interaction. Cross section *σ* has the dimensions similar to an area of single nucleus. Since the effective size of the nucleus is extremely small, a suitable unit is introduced called *barn* with following size [3]:

$$1 \, \text{barn} = \ 10^{-28} \, \text{m}^2. \tag{3.5}$$

For a single neutron the probability of every interaction differs and has its own cross section with lower indexes signifying the type of a reaction, and all of them are related to the energy of the neutron. For example, the cross section for elastic scattering of a neutron on a nucleus is symbolized as $\sigma_{n,n'}$.The type of resulting reaction depends on neutron's energy, dividing cross section into two major groups – capture cross section and scattering cross section. If we want to calculate the total cross section for the number of nuclei *N* per unit volume, it equals [3]:

$$\Sigma = N\sigma, \tag{3.6}$$

and is sometimes called as *macroscopic cross section Σ*, and its dimensions are of inverse length. Also in this case the macroscopic cross section is defined for every interaction, therefore the total macroscopic cross section Σ_{tot} is a summary of all processes combined together [3]:

$$\Sigma_{\text{tot}} = \Sigma_{\text{scatter}} + \Sigma_{\text{neut. capture}} + \cdots. \tag{3.7}$$

Σ_{tot} then actually expresses the probability per length that a neutron undergoes any possible interaction.

The number of detected neutrons decreases exponentially when entering a matter and the behavior has a parallel in the absorption of beta and gamma radiation [3]:

$$I = I_0 e^{-\Sigma_{\text{tot}}t}. \tag{3.9}$$

Particularly for reactions induced by neutrons the concept of neutron flux should be put forward to eliminate inaccurate geometry of neutron interactions, since their path is not collimated into a single line beam, but they are chaotically emitted in all directions when coming from a source or when neutrons are scattered after an encounter with a nucleus. For monoenergetic neutrons with a constant velocity v and neutron number density $n(r)$, which is a function of vector position $\boldsymbol{r}$, the neutron flux is defined as [3]:

$$n(\boldsymbol{r})v = \varphi(\boldsymbol{r}); \ \ [\varphi(\boldsymbol{r})] = \mathrm{m}^{-2}\mathrm{s}^{-1} \tag{3.9}$$

The reaction rate density, described as reactions per unit time and volume, is then defined as:

$$RRD = \varphi(\boldsymbol{r})\Sigma, \tag{3.10}$$

where Σ is previously mentioned macroscopic cross section. Like the cross section, neutron flux is energy dependent as well, so a generalization can be made by using $\Sigma(E)$ instead of Σ, and $\varphi(\boldsymbol{r}, E)$ instead of $\varphi(\boldsymbol{r})$ [3] :

$$RRD = \int_0^\infty \varphi(\boldsymbol{r}, E)\Sigma(E)dE. \tag{3.11}$$

Cross section plays an important role in NAA. Based on the neutron's energy and cross section, predominantly the capture cross section, the most possible interaction between a neutron and nucleus can be determined. This information suggests which reaction is key for us. The knowledge of the reaction can be later used for specifying the character of radiation emitted from activated material (see Chapter 6). A convenient online tool called ENDF (Evaluated Nuclear Data File) [22] accessible through a website www.nndc.bnl.gov/endf/ can be used to view plots and browse other information. By typing in the required element and optionally a reaction, a database opens up containing all the useful information. The database itself is also categorized and cross sections for various analytical methods can be viewed, for example, cross sections for prompt gamma rays from activated materials. For example, the Figure 3.5 shows the cross section for (n,2n) reactions on [56]Fe and how the cross section relies on neutron's energy and that the most suitable neutrons for (n,2n) reaction are those with energy of 14 MeV [22]:
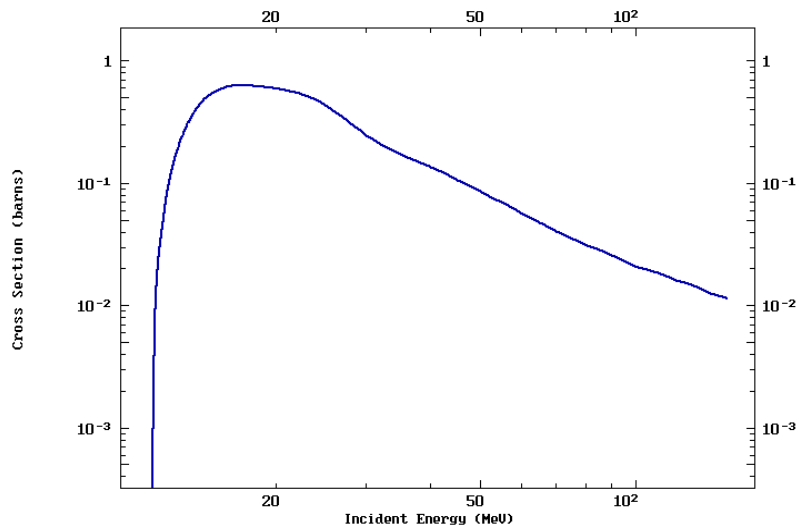
Figure 3.5: A plot expressing the cross section of the reaction (n,2n) on ⁵⁶Fe with relation to incident energy.

3.3 Protection Against Ionizing Radiation

This section will concern options of shielding and other safety measures reducing the danger of ionizing radiation. All of us are exposed to a small dose of radiation coming either from space as *cosmic radiation* or natural sources. This radiation is called **background**, but since the background radiation doesn't significantly endanger us, it will not be a subject to us. We are going to focus on ionizing radiation that could stand a potential risk for our health, or it could affect measurements done with detectors [3].

3.3.1 Radiation Shielding

The most simple and yet crucial way of minimizing the ionizing radiation effects is by shielding the source. Because alpha and beta radiation are rays of particles, which are shielded with ease due to their mass and charge, no difficult to produce materials have to be used to completely shield the radiation. However, gamma-rays deeply penetrate any matter, therefore specific materials have to be used and appropriate properties must be taken into consideration to create a safe environment [5].

Concrete, lead and steel are widely used materials for shielding. All three of these have a high density and a high atomic number in common. 10 centimeters of lead can completely shield off gamma radiation, but its price and availability tip scales in favor of cheaper options. On the other hand, concrete is the low cost option from these three materials, but its width must be at least one meter to be able to shield off most of the gamma radiation. In general, the thickness of a shielding is a pivotal property and must be assessed before committing to choosing a material. For neutrons, the shield is required to absorb both gamma-rays and neutrons. Because neutrons penetrate the matter deeper than gamma-radiation, the width of the shielding should be capable of absorbing neutrons as well [3].

Figure 3.6: Shielding at VŠB-TU Ostrava; the wall was created with YTONG blocks to shield incoming neutrons.

3.3.2 Personal Protective Equipment

Exposure to ionizing radiation can take a huge toll on one's health. Tissue and organs exposed to radiation can be damaged because their cells are dying when being irradiated. The protection of our health against ionizing radiation is then more a subject of prevention than active protection gear. The safety standards and recommendations are set internationally by IAEA (International Atomic Energy Agency) or by each country's government. These limits are set so workers, scientists and the general public are not put in danger when they are long term exposed to radiation [23].

For active protection, distance, time and shielding are the three main protective measures reducing the effects of ionizing radiation. Personal protective equipment (PPE) is used to reduce the risk of exposure. PPE includes clothing such as gloves, headgear, bodysuits, etc., or detectors and other tools providing actual information about radioactivity in the user's vicinity. Also various safety courses are usually carried out in places, where there is a risk of exposure to radiation, to train people how to prevent themselves from harmful exposure and how to act in emergency situations as well [24]. Principles of radiation detection are discussed in the following section.

3.4 Radiation Detection

In the past decades technology went through a huge advancement and so did science. New physics discoveries with the help of computers and other technology have opened up new ways of observing physical phenomenons. Simple detectors with many disadvantages were replaced by sophisticated automated detecting systems to provide more information about the measurements and to make results more superior as well [26].

3.4.1 Basics of Radiation Detection

The essential event for a detecting system to detect any kind of radiation is its interaction with the matter of the detector. The matter of detector is called *medium* and sometimes there is an adjective connected to it - *active medium*, which means that the matter has a dominant amount of atoms or molecules which can undergo an excitation or ionization, in other words, it is possible to observe a transformation of radiation energy to the matter. These two processes are used in the most common detectors [26].

The second part of a detector is the readout *system*. Physical changes in the matter after an interaction with radiation generate signals in the readout system which are then analyzed and compiled in an computing unit [25]. The simplest readout systems analyze signals emerging from the change or formation of an electric charge in an electric field within the detector. The time between an interaction and collection of the signal is then one of many properties describing the quality of a detector [3]. Various detectors can perform multiple tasks, for example [25]:

- Particle tracking
- Particle identification
- Energy determination
- Data acquisition

In general, detectors are able to analyze a plenty of properties, but the quality and precision of these measurements vary from detector to another, therefore is it essential for an experimentator to understand the functions and limits of each detector type [25]. It is also possible to perform a measurement in several different modes, making the analysis easier and more efficient, but we can meet with more measurement uncertainties resulting from an effect of *dead time.* Dead time is a minimum time between two separate events, which can be analyzed. If the time between those two events is shorter than dead time, the detector could analyze these events as one. Dead time is another detector property which should be considered when performing a measurement [3]. Types of detectors and their usage will be treated in the following section.

3.4.2 Examples of Radiation Detectors

The use of detectors is diverse. For each radiation type one group of detectors is more adequate than the others, some detectors can only detect particles, whereas some complex detecting systems can also track and identify what particle it is and so on. To briefly narrow down these detector capabilities, we should take a look at some of the widely used types of detectors there are:

- **Ionization chambers** are the simplest and oldest detectors and make use of ionization produced in a gas. The chamber of the detector is filled with gas that can be ionized after a charged particle passes through the gas and the formation of an electron or ion pair is then collected by the readout system [26]. Ionization in gasses is also used in Geiger-Müller or proportional counters, where the charge produced from the formation of ion pairs is increased by gas multiplication to enhance the detection [3].

- **Semiconductor detectors** contain the active medium in solid state. Signals for the readout system are created by electron-hole pairs, which form along the path of the charged particle in the medium. The principle is analogous to the ion pair formation in an ionization chamber, but semiconductor detectors are more beneficial, because the same effect can be achieved in way smaller size of the medium [3]. Also in comparison with ionization chambers, the semiconductor detectors operate faster and the energy required to create an electron-hole pair is lower [26].

- **Scintillators** are detectors where the active medium is made out of luminescent material. When ionizing radiation passes through the medium, a population of excited states of electrons is formed which then immediately decays by flash of light (scintilation). These scintilations are then trapped and multiplied in a photomultiplier tube to produce an electric signal to the readout system. We are actually able to see some sort of visual outcome of the interaction in the form of a faint flash [27].

- **Photographic films** are made of an emulsion that changes its chemical composition when encountering ionizing radiation. The film is then developed and the path of a particle is visible as a darkening of the film. It is quite difficult to identify the incident particle, but its path is visible by naked eye, so that's a huge advantage to this detection method. Photographic films are widely used for personnel radiation-dose monitoring [27].

- **Calorimetry** is based on an ionizing radiation energy transformation into heat in the medium. Since the increase in temperature is extremely low (e.g. 1 °C temperature rise in water is equal to an absorbed dose of 4180 Gy), calorimeters are used to measure absorbed doses given by high-intensity radiation. Calorimetres also have to be perfectly insulated to prevent the apparatus from measuring heat from the outside of the system [27].

- **Cherenkov detectors** make use of the Cherenkov effect. When a charged particle passes through a matter with a velocity higher than the speed of light in a given medium, it emits an electromagnetic radiation along the path of the particle. It is visible as a blue glow in the medium and it can be occasionally seen in reactor cores. The effect is analogous to the shock wave produced in air when an object travels at the velocity higher than the speed of sound [27].

- **Neutron detectors** work on a different basis than detectors of ionizing radiation, due to the fact that neutrons do not ionize or excite the matter when interacting with it. Neutron detectors employ nuclear reactions and detection of their products, principally charged particles. The neutron cross section is related to neutron's energy, hence the detection system and the target material is constructed in a way to detect neutrons of particular energy, which means that for detection of slow neutrons some target materials are more appropriate than for fast neutron detection [3].

4.   Gamma Spectrometry

For the study of energy spectra of gamma-ray sources (in my bachelor thesis it is by neutrons activated materials) methods of gamma spectrometry are used. Gamma spectrometer contains a detector and electronic device for the analysis of the detector's output signals. Spectrometry method can be done using either semiconductor detectors or scintillation detectors. Since my bachelor thesis wraps around a scintillation detector, semiconductor detectors are not a subject to our description.

4.1   Introduction

Scintillation gamma spectrometry makes use of scintillation in solid crystals, which is used as a detection medium. It is considered to be the one of the best detector types to measure radiation because of its good energy resolution and variety of functions that can be used. One of scintillation detection's dominant advantages is the ability to measure every radiation type – alpha and beta particles, neutrons, but most importantly gamma rays. We will only focus on gamma spectrometry in further description, which is used for determination of individual radionuclides in gamma emitters [6].

4.2   Principle of Detection

For a detector to detect gamma radiation, the radiation must interact with atoms of the medium, where photons transfer their energy to electrons, which are then "torn off" from atoms and lose their energy by ionizing the medium or exciting nuclei in its vicinity. Since these electrons have a maximum energy equal to the energy of incident photons, the determination of a photon's energy is therefore a matter of calculations and analysis. From all the possible interactions between the atom and photon, three of them have a major significance in the spectroscopy – photoelectric absorption, Compton scattering and pair production. Each interaction mechanism is more probable than the others in a given energy range. For energies lower than a few hundred keV the photoelectric absorption is the most significant, for energies above 5 MeV the pair production is the most probable and Compton scattering fills the gap between those two processes. The processes have already been featured in subsection **Interaction of Gamma Rays with Matter** (see section 3.1.3), thus only a brief description of how the energy from the process is detected follows [3]:

- Photoelectrons formed after **photoelectric absorption** carry the same energy as the original photon. Because of this fact, the photoelectric absorption is considered to be the fundamental interaction for gamma spectroscopy, because only single energy peaks appear in the *spectrum* (see Section 4.4) which corresponds completely to the energy of incident gamma radiation and no fluctuations of significance take shape [3]. The Figure 4.1 [3] represents the formation of peak given by the photoelectric absorption. We should note that radionuclides do not emit gamma rays of a single energy at all times, numerous nuclides emit gamma-rays of multiple energies, therefore more peaks appear in the spectrum.

Figure 4.1: Distribution of energy given by photoelectric absorption.

- **Compton scattering** is way more complex interaction that produces recoil electrons after a scattering of photons. Because the energy of formed electrons and scattered photons depends on the angle of scattering, a continuum of energies, usually called Compton continuum, is measured and the distribution of electron energy can also be depicted as shown below in Figure 4.2 [3].
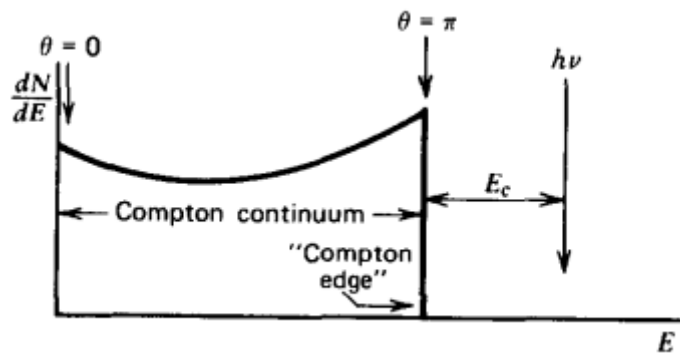
Figure 4.2: Distribution of energy given by Compton scattering.

In comparison with previous depiction, the difference is obvious and energy distribution contains a lot of fluctuations due to other effects of the scattering of low energy gamma-rays [3].

- In **pair production** positrons and electrons are formed. For this interaction to be possible, an energy of 1,02 MeV is required. Both of these particles ionize the material therefore the scintillation occurs. Positron is unstable and annihilates with electron, producing two or three photons with overall energy of 511 keV [17]. In the whole spectrum the pair production energy peaks appear as a *single escape peak* located m_0c^2 below the incident photon energy, or *double escape peaks* located $2m_0c^2$ below the incident photon energy [3].

In order to understand how the materials of detectors influence the measurement, a brief description of the construction of the detector follows.

4.3   Spectrometer Materials

The scintillation material must meet several requirements to be useful in spectrometry. The most important are [3 - 6]:

- Ability to convert the energy of charged particles into detectable light.
- High density and atomic number (creates high stopping power for gamma rays).
- The response must be proportional to the energy of gamma-rays.
- The decay time of excited states is short so fast signal pulses can be generated.
- The material must be transparent.
- Good optical quality is maintained even in larger sizes.

There are a few of these crystals that are able to fulfill the requirements, but to this day, the most generally used is a sodium iodide crystal NaI(Tl). The NaI(Tl) crystal is cheap, available and has many dominant properties, which makes it more preferable than other crystals. For example, the number of photons emitted per unit of gamma-ray energy absorbed by the crystal is called *light output* and for the NaI(Tl) crystal the value stands at 38 000 photons per MeV. Other materials are then usually compared to NaI(Tl), referred to as *relative conversion efficiency* and their efficiency is expressed in percentage. NaI(Tl) also has the highest energy resolution from all the scintillation crystals, but on the other hand, its high sensitivity to temperature and hygroscopic character create a difficulty in its production and operation [6].

In general, the detector's size is greatly relevant when we intend to eliminate the influence of secondary radiation. Another aspect would be the detector's shape. For a good light output and simplicity, the crystal is most often shaped into a cylinder [3].

4.4   Data Collection

The process of collection and analyzing the data is intricate, so a simple and brief description follows to point out important parts of the procedure. All the energy from interactions is outputted as a quantity of light in the crystal. The light is then converted into an electric signal, which can be done using *photomultiplier tubes* and enhanced using *amplifiers*. These multiple enhanced signals are then analyzed and collected by *Multichannel analyzer (MCA).* MCA's task is to measure the count and height of signal pulses and all these increments are then combined and overlapped to shape a histogram or so called *energy spectrum* [17]. The spectral shape given by a single gamma-ray, called response function, is highly dependent on various properties, predominantly the detector's size, incident gamma-ray energy and materials surrounding the detector. As an example for description of spectrum I will use one that I have measured in a laboratory at VŠB-TU Ostrava, Czech republic, where we used an isotope Cs-137, for which the spectrum is simple and convenient to describe. Cs-137 emits gamma-rays with energy of 661,657 keV [28].
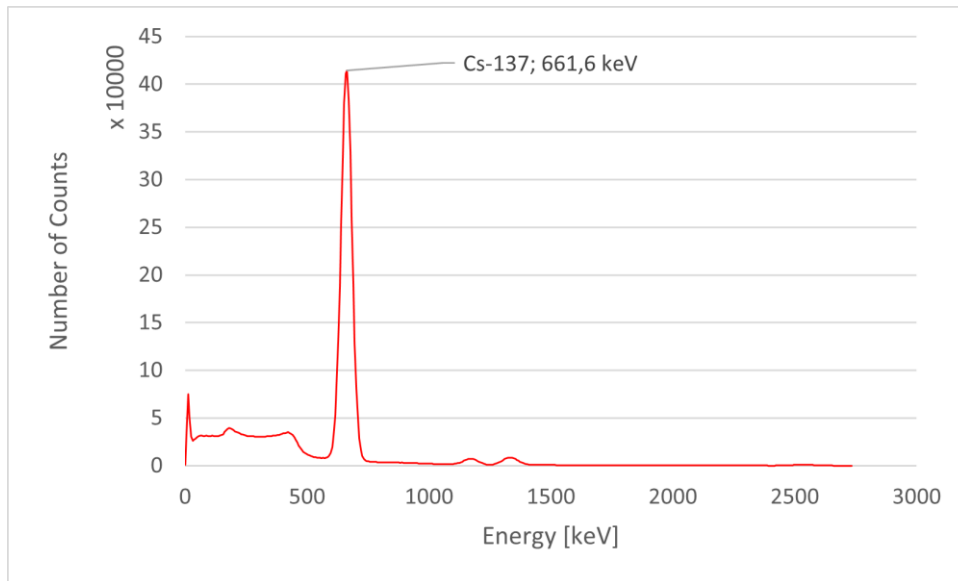
Figure 4.3: The spectrum of Cesium-137.

As we can see, the number of counts of Cs-137 is dominantly outnumbering the counts of background and thus the single peak of Cs-137 appears. In the energy range of 0 to 500 keV the Compton continuum can be seen.

Gamma emitters emit photons with one or more energies, which can be seen in a spectrum as a peak in given energy value. To find out how radioactive nuclides decay and to determine their photons energy, nuclide databases and decay schemes are used [17]. One of the most widely used databases is owned by IAEA and can be used in various interactive forms. The most convenient is probably the interactive nuclide chart, which is accessible online at IAEA offical website, where one can simply click on a nuclide of his choice and gather useful information about it, where key for us is the *decay scheme.* Decay schemes serve as an illustration of how the specific nuclide decays. Different energy levels are seen with description of the probability for the nuclide to decay by this mean also with the amount of energy emitted during this decay [6]. For example, if we take a look again at the decay of Cesium-137, its decay scheme is shown in Figure 4.4:
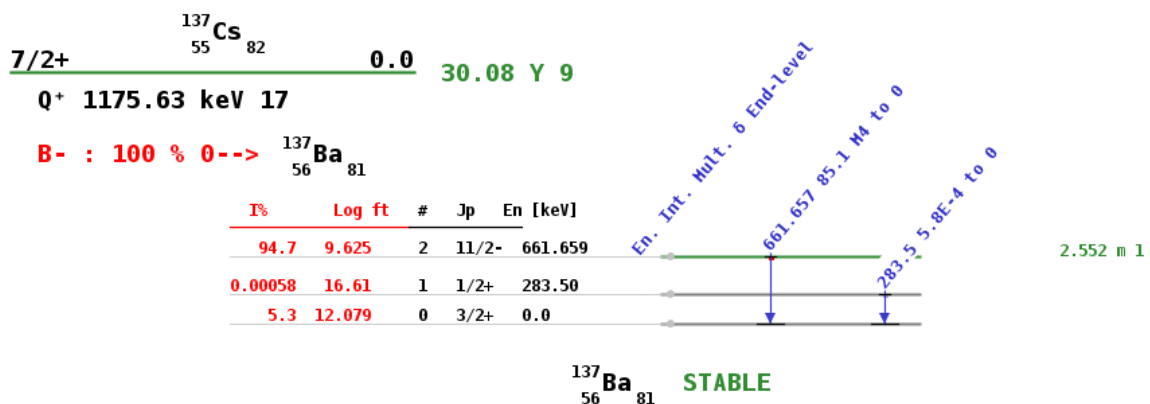
Figure 4.4: The decay scheme of Cesium-137.

One can notice that 100% of the Cs-137 decays by β⁻ emission to metastable Ba-137m, which then immediately decays by emission of required gamma-rays with energy of 662 keV. Unfortunately, decay schemes may sometimes be really complicated to understand and difficult to orient in, therefore I prefer to use a nuclide library on a site Nucleide.org [28], where important information is summarized in straightforward tables. Again, for Cs-137, the Table 4.1 (data from Nucleide [28]) lists energies of gamma-rays. In comparison with the decay scheme of Cs-137, the table is more organized and simple.

	Energy (keV)	Photons per 100 distint. [a]
$\gamma_{1,0}$(Ba)	283,5	0,00058
$\gamma_{2,0}$(Ba)	661,657	84,99

Table 4.1: Energies of gamma-rays emitted by Cesium-137 from nucleide.org.
[a] can be interpreted as the probability of emission.

Decay schemes and the knowledge of energy levels can serve many purposes. Computers connected to measuring apparatus are able to perform specific analytical methods that process spectrum and give out useful information. For instance, there are algorithms that are able to locate peaks and determine their energy, which are then processed with a use of nuclide libraries to reveal the nature of the peak and assign this peak to an original element, therefore a complete evaluation of unknown gamma emitter can be done [17].

In order to convert the data collected in the spectrum into an activity of the sample, a calibration of the detector has to be done.

4.5   Energy and Efficiency Calibration

Certain procedures and calculations can be carried out to eliminate measurement errors. They are called "calibration" and two main calibration methods are subject to our following discussion [17].

Energy calibration expresses the transformation of channel numbers into energy values. By measuring the spectrum of a gamma-ray source with precisely known energy values we are able to compare the measured peak with the real energy value and get rid of the difference. The choice of the source usually depends on how many peaks the experimentator wants to work with and whether he wants a source with single or multiple nuclides [6]. Certified sources with sufficient probability of emission and long half-life can be purchased and contain information about their activity according to a specific reference date. The commonly used standards are Eu-152 and Ba-133, but mixed standards are available as well and serve for a measurement of a wider range of energies [17]. A long measurement is better to be done for statistical precision. Once the measurement of the standard is finished, a computer analysis determines the position of the peaks assigned to channel numbers and a two point linear calibration is usually carried out [6]:

$$E(keV) = I(keV) + G \times C(channel), \qquad (4.1)$$

where *I* and *G* are determined using regression analysis and *C* is the number of channel. When the calibration is complete, the energy is assigned to correct channels and we may expect no further errors

in measurements. For a more precise calibration, other methods, such as multi-point nonlinear calibration, can be done as well [6].

   Efficiency calibration expresses the relationship between the number of counts and disintegration rate. The relation between the total number of counts detected in the whole spectrum (Compton continuum is taken into consideration too) and the number of gamma rays emitted by the source is called *absolute total efficiency*. In comparison with relative and intrinsic efficiency, the absolute total efficiency is the one of greater significance. Efficiency is influenced by various factors such as source-to-detector distance, shape of the source, absorption within the source and so on, but it also correlates with the energy, so a full calibration of the detector is needed. In practice, a full-energy peak efficiency is the most important parameter, from which we are able to gather the information that concerns us. The principle is simple, the full-energy peak efficiency puts the number of counts detected in a peak and number of gamma rays emitted by the source into a ratio [6]:

$$\varepsilon = \frac{R}{AP}. \tag{4.2}$$

R stands for the full-energy peak count rate given by counts per second, *A* is the activity of the source and *P* is the probability of emission of the gamma-ray. Again, a certified source with a reference date should be used so the activity in the time of measurement can be specified, because as we know, the activity of radionuclide with short half-life decreases after time. By a simple operation, an equation for the calculation of the activity of the source can be formed [6]:

$$A = \frac{R}{\varepsilon P}. \tag{4.3}$$

5.   D-T Neutron Generators

There are several types of sources of neutrons. There are natural sources, where neutrons are generated as a product of certain reactions of radionuclides, but there are also man made sources, such as nuclear reactors, D-D neutron generators and D-T neutron generators. D-T neutron generators are based on the D-T reaction, which occurs between deuterium (D) and tritium (T) [3]. Before we explain the theory behind this neutron generation, we should shine some light on the deuterium and tritium themselves.

5.1   Deuterium and Tritium

Both deuterium and tritium are isotopes of hydrogen, though only the tritium is radioactive. Deuterium is commonly symbolized by the letter D instead of ^{2}H and so is for tritium, for which is used the letter T instead of ^{3}H. As we can see, deuterium has 1 neutron in its nucleus and tritium has 2 neutrons, consequently making the tritium unstable. We should note that deuterium is extremely rare in nature, but is able to substitute the hydrogen in H_2O molecules resulting in formation of D_2O, which is called "heavy water" [29]. The unstable tritium has a half-life of 12,26 years and decays to ^{3}He by emitting beta radiation. The energy of the beta particles range from 5,7 keV to 18,6 keV. Tritium is also able to form T_2O molecules or so called "super-heavy water". The tritiated water is radioactive and finds its utilization in a method of measuring the total volume of water in the human body, although its effects on one's health should be taken into account [30].

5.2   Principle of Operation

The D-T generator produces neutrons from a D-T reaction. In this reaction, deuterium ions are accelerated by a potential in the order of tens to hundreds of kV and tritium serves as a light target nucleus. The nuclear reaction is often symbolized as ^{3}H(d,n)^{4}He, signifying that the tritium comes in interaction with deuteron as shown below [3]:

$$D + T \rightarrow {}_2^4He + n + 17,6 \text{ MeV}. \tag{5.1}$$

The initial D + T reaction produces unstable ^{5}He which then either decays to ^{4}He, followed by an emission of the excess neutron, or results in two other possible reactions [13]:

$$D + T \rightarrow {}_2^3He + 2n - 2,988 \text{ MeV}, \tag{5.2}$$

$$D + T \rightarrow T + p + n - 2,225 \text{ MeV}, \tag{5.3}$$
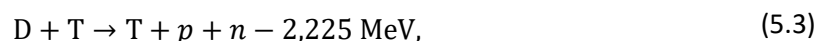
but their cross sections are low due to operation conditions, therefore in practice they are insignificant [13]. In the Eq. 5.1 the *Q*-value is distributed between the kinetic energies of the produced alpha particle, which has an energy of about 3,5 MeV and the rest of the total energy, 14 MeV, makes up the energy of the neutron [3]. A schematic representation of interaction between deuterium and tritium is shown in Figure 5.1 [17].
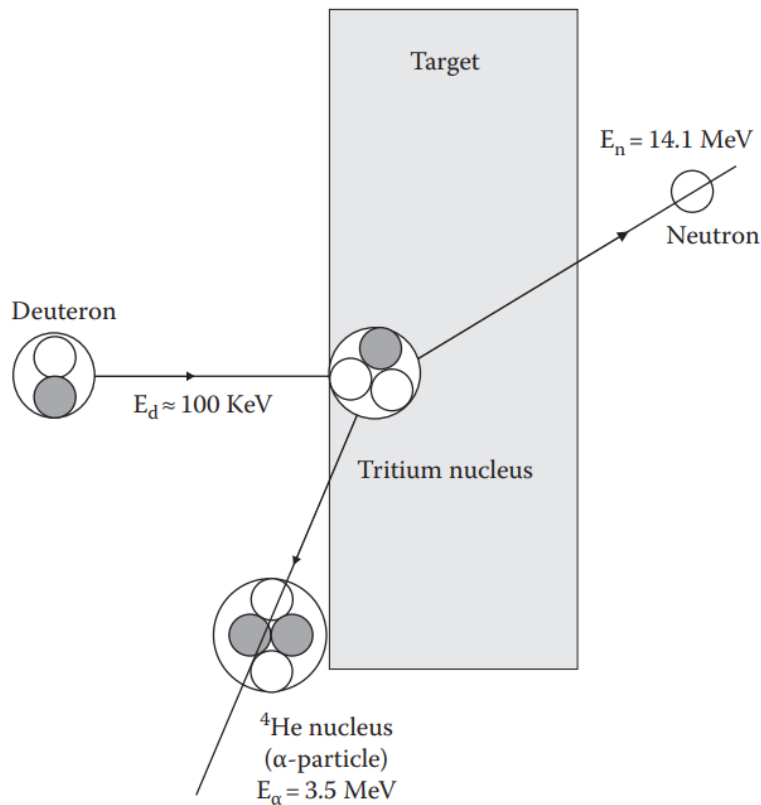
Figure 5.1: The scheme of interaction between deuteron and target tritium.

The neutron generator itself usually comes in many forms, but the most common type of generator is in the shape of a sealed tube and is composed of the ion source, a region used for accelerating ions and a target section, where the tritium is and the fusion reaction takes place. Some generators are able to operate in two modes - a continuous mode or a pulse mode. Pulse mode allows the production of neutrons in frequency up to tens of kHz, which is useful for cycling the activation of materials in NAA (see Section 6.2). Neutrons produced from the D-T reactions are emitted into all directions (4π sr) and produced alpha particles always travel in the opposite direction of the neutrons, therefore a sufficient shielding is required in an effort to form a collimated beam of neutrons [13].

5.3   Utilization

An ongoing world-wide study suggests that the fusion process of deuterium and tritium could be exploited in order to make a great quantum of energy compared to the low activation energy of the reaction and is achievable by using very light elements instead of using fissionable resources such as Uranium-238. A development of a special device called "tokamak" is in progress and is assumed to be able to convert the energy of alpha particles created in the fusion process into heat, which would then be used to power generators and create electricity [13].

Thermonuclear power is not in our interests, but we find utilization of neutron generators in neutron activation analysis, for which its principles are described in the following section.

6.   Neutron Activation Analysis

Neutron Activation Analysis is an analytical technique widely used for sample analysis. Main object of this method is a complete identification of elements present in a given sample both qualitatively and quantitatively. What gives the NAA the upper hand in comparison with other analytical methods is its high sensitivities and ability to identify even a slight amount of trace elements in the sample. Considering the dangers of manipulating with neutron sources and ionizing radiation and also the availability of instruments used for this method, the NAA is performed only in special laboratories with such equipment and performed by highly educated and experienced workers [31].

After the discovery of neutrons by J. Chadwick in 1932 a widespread urge to follow the path of Chadwick appeared amongst scientists and a race to develop new possible techniques and experiments began. The primacy of discovering the NAA method belongs to **Hevesy** and **Levi** after they discovered that samples containing a rare earth element, dysprosium, became highly radioactive after an exposure to neutron source. This principle is the base of neutron activation analysis [32].

6.1   Theory and Principle

NAA is a non-destructive method of sample analysis and samples do not need to be prepared in any way. After putting the sample in the apparatus it is irradiated by highly thermalized neutrons generated by reactors or generators that were mentioned earlier (see Section 5). During the irradiation, elements in the sample are transformed into their unstable radioactive isotopes by neutron capture. The reaction is often symbolised as (n, γ). If we observe the reaction more in depth, we can see that the neutron comes into a nonelastic collision with the target nucleus and a compound nucleus is formed. Instantly the compound nucleus dexcites into a stable form through emission of one or more characteristic prompt γ-rays. These formed isotopes have half-lives ranging from seconds to years. In many cases the new configuration is also radioactive and decays by emission of one or more delayed γ-rays. Therefore NAA is split into two categories with respect to the time of measurement: PGNAA, or Prompt Gamma NAA measures the emission of γ-rays during the irradiation and DGNAA, or Delayed Gamma NAA, where delayed γ-rays are measured, as seen in Figure 6.1 [31].
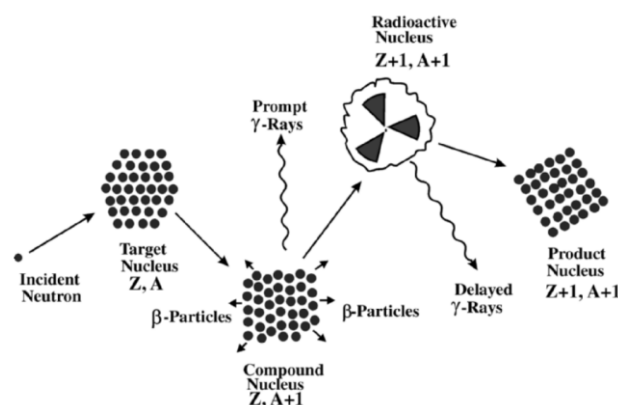

Figure 6.1: The schematized principle of PGNAA and DGNAA.

PGNAA makes use of external generator of neutrons to irradiate a sample which then decays by gamma emission with energies and cross sections characteristic of all elements and the analysis is performed simultaneously with the irradiation, whereas DGNAA is more sensitive to gamma-rays emitted by radioactive isotopes with longer half-lives, which are measured after radionuclides with short half-lives completely decay [31].

6.2   FNAA and Connection with my Thesis

Another branch of NAA, the Fast Neutron Activation Analysis (FNAA) is what concerns us to obtain gamma-rays of higher energies. FNAA utilizes activation of samples with 14 MeV neutrons generated in D-T generators. Radioactive isotopes with comparable short half-lives and high energies are produced. Though, a major problem occurs when one wants to measure energies of those short half-life radionuclides – stastically one measurement does not provide sufficient amount of counts, therefore the analysis of the sample is not reliable and the contribution of background radiation also makes an impact on the data in a spectrum. A little change in the method of operation makes the results more correct and higher sensitivity is achievable. If the sample is irradiated in repeated cycles, every single cycle activates the sample to saturation. The background radiation then increases slower compared to the increase in the number of counts of characteristic gamma-rays. Spectra of every cycle is then added together to shape one final spectrum. The spectrum is strongly dependent on the acquisition setup and choice of cycle interval and total time of measurement. Sometimes, the measurement with set pulses is called Pulsed Fast Neutron Analysis (PFNA), or when thermal neutrons are involved it is called Pulsed Fast and Thermal Neutron Analysis (PTFNA), but these names are usually used accordingly to the setup of apparatus [13].

We have mentioned that neutron generators are able to operate in pulse modes, thus in FNAA that option plays the key role. Furthermore, the spectrometers can be controlled by external input, so when connected directly to the generator, the spectrometer is capable of measurements in frequencies up to tens of kHz. It is better to perform several measurements to tweak and find a sufficient cycle length to avoid measuring high background radiation, possible effects of interactions of delayed neutrons coming from the source and, from our own experience, a high detector dead-time [13]. Energies of activated nuclides can be found in various databases, but mainly IAEA databases are used because they are updated frequently, therefore are always up-to-date.

6.3   Activation of H, C, N and O Elements

Activation of these elements serves two purposes in our interest. The use of 14 MeV neutrons for activation of hydrogen, carbon, nitrogen and oxygen leads to emission of gamma-rays with energies above the highest energy levels of gamma-rays of natural radionuclides and typical calibration standards which are in order of 1 to 3 MeV. For example, K-40 with a half-life of $1,29 \times 10^9$ years decays with gamma-ray energy of "only" 1461 keV. Th-232, another nuclide participating in the background radiation, has a dominant energy of 2,614 keV [28]. In contrast with energies of H, C, N and O prompt gamma-rays after being activated by both 14 MeV neutrons and thermal neutrons, we can observe that these energies are way above the K-40 or Th-232 energy level, as shown in Table 6.1 (data from [33]).

Element	Energy (MeV)	Incident Neutron
H	**2,2232**	Thermal Neutron
	1,2618	Thermal Neutron
	3,6839	Thermal Neutron
C	**4,4390**	Fast Neutron
	4,9453	Thermal Neutron
	0,7284	Fast Neutron
	1,6353	Fast Neutron
	1,8848	Thermal Neutron
	2,3128	Fast Neutron
	2,7931	Fast Neutron
	3,3786	Fast Neutron
N	3,8907	Fast Neutron
	4,9151	Fast Neutron
	5,1059	Fast Neutron
	5,2692	Thermal Neutron
	6,4462	Fast Neutron
	7,0291	Fast Neutron
	10,8291	Thermal Neutron
	0,8707	Thermal Neutron
	1,0879	Thermal Neutron
	2,1845	Thermal Neutron
O	2,7420	Fast Neutron
	6,1299	Fast Neutron
	6,9171	Fast Neutron
	7,1168	Fast Neutron

Table 6.1: List of characteristic prompt gamma-rays for H, C, N and O. Bold font was used for gamma-energies typically used to characterize the element.

Besides these four listed elements, other elements such as Al, Fe, etc., which are present in the environment of the laboratory, can be activated by 14 MeV or thermal neutrons as well. On account of the activation and capability to reach higher energies, the energy calibration of the spectrometer in the high-energy level is realizable. Notable are half-lives of these activated nuclides, ranging from seconds to minutes (eg. ^{16}N decays with a half-life of 7,13 s), implying that the measurement should be performed in cycles to gather adequate data for correct analysis and calibration [13].

The second purpose is the role of these elements in NAA applications. H, C, N and O elements are essential for the composition of organic compounds, to be more specific – urea chemical compounds are those in our attention. Rationally, explosives are not available to the public or schools, so urea serves as a convenient substitute and also urea can be used to calibrate detectors used for this method. Urea is chemically similar to the composition of explosives (especially urea nitrates are explosives themselves). We've used urea standards with intention to simulate the detection of

explosives using the NAA method. When the samples of urea or explosives are bombarded with neutrons, induced nuclear reactions are used for the detection of elements, concentrations and concentration ratios, which then indicate if the sample is either explosive or other chemical compound [13]. Every explosive chemical compound has a specific mutual ratio of element concentration or so called "stoichiometric formula". In the Table 6.2 two examples of such formulas are listed (data from [34].

	N (weight in %)	O (weight in %)	C (weight in %)	H (weight in %)
C-4	30,26	41,71	24,35	3,68
PL SE M	29,88	39,73	26,38	4,01

Table 6.2: Stoichiometric formulas of American plastic device of type C-4 and Czech plate explosive PL SE M.

Unknown analysed samples are then compared to explosives with known ratios of elemental representation in the sample and besides the ability to detect the explosives, it is also possible to quickly determine the type of explosives. This method is widely used at airports or at customs borders, but due to cost of the used equipment and required skill and knowledge, other methods are performed instead [34]. The detection of explosives is one of many applications the NAA method can provide. In the following section further applications are discussed.

6.4   Applications

One may say the rise of terrorism in the world is the reason for the growth of neutron activation analytical method. After numerous terrorist attacks, involving the deadliest one, the 9/11 attacks on WTC, homeland security changed from the ground up. All countries around the world have put a huge amount of money into the development of security precautions, detection systems and so on. The illegal explosives, drugs and nuclear material trafficking internationally grew and border management were forced to keep up with the growth by developing quicker and more sensitive methods of detection [13]. New methods were developed, including NAA, and their applications spread out into other areas of research. Besides the detection and identification of explosives using NAA, other applications can be seen nowadays [31]:

1. **In archeology:** a method called "artifact fingerprinting" serves for determining the source of materials that found artifacts were made of
2. **In biochemistry:** radiotracers produced by neutron activation are used to study biochemical processes in the small animal model; determination of concentration levels of Se and mineral nutrition aspects of human health
3. **In ecological monitoring:** study of the concentration of toxic heavy metals in industrial type air particulates; study of uranium representation in mine waters; etc.
4. **In microanalysis of biological materials**: analysis of hair, nails, blood, …, for toxic trace elements
5. **In forensic investigations:** analysis of extremely small evidence samples
6. **In geology:** study of processes that are behind the formation of rocks through activation of rare earth elements and trace elements
7. **In material science:** detection of components of metals, semiconductors and alloys
8. **In food industry, agriculture, soil science** and many more

7. Measurement Apparatus

In this chapter I will introduce the measurement equipment and configuration that was used for the data collection. Every component and its settings and specifications are listed in each section and at the end of the chapter the whole setup and the role of each component is summarized.

7.1 MP320 D-T Neutron Generator

A company Thermo Fisher Scientific supplied our laboratory with a MP320 D-T Neutron Generator that generates 14 MeV neutrons with a high neutron yield of 10^8 n/s from deuterium and tritium fusion. The generator is capable of operation in continuous mode or generating neutron pulses in the range of 250 Hz to 20 kHz, which is suitable for PFNA. The generator also comes with an electronics case with a built-in power supply to accelerate particles in the accelerator tube with an electric potential of 95 kV maximum [35].

Figure 7.1: MP320 D-T Neutron Generator used at VŠB-TU Ostrava.

The case allows us to connect a detector or other devices via special cables to output both immediate pulses and delayed pulses. Also, it is possible to externally control the generator when it is connected to another device through a "CONTROL" port. Besides this option, the generator is controlled digitally with a software that comes with the generator. This machine is mainly used for the detection of explosives, chemical weapons, buried landmines and drug detection. Important characteristics of MP320 D-T Neutron Generator are summarized below [35]:

Neutron Yield	10^8 n/s
Neutron Energy	14 MeV
Pulse Rate	250 Hz to 20 kHz
Duty Factor	5% to 100%
Maximum Accelerator Voltage	95 kV
Beam Current	60 μA
Minimum Pulse Width	5 μs

Table 7.1: Summary of some properties of MP320 D-T Neutron Generator.

7.2   NaI(Tl) Spectrometer

The gamma spectrometer consists of a scintillation crystal from natrium iodide doped with thallium. It was supplied to our laboratory by a dutch company Scionix Holland. This detector stands out for its size, as standard scintillation detectors are in a shape of a cylinder and have a length of 7 inches (177 mm), this NaI(Tl) scintillation crystal has dimensions of 76×127×406 mm and weighs around 15 kg. The housing of the detector is made of 0,8 mm stainless steel. A photomultiplier tube with a diameter of 76 mm is joined to the crystal and has an ethernet port and 3 GPIO ports for input [36].

Figure 7.2: NaI(Tl) Spectrometer produced by Scionix Holland.

The spectrometer contains a multi-channel analyzer MCA that is connected via ethernet cable to the computer. A convenient software to use is Genie 2000 Basic Spectroscopy software, which is able to acquire and display data, analyse the obtained spectra and initiate custom algorithms and scripts using a software development kit that comes with the software [36].

7.3   Urea Standard

The urea standard NH_2CONH_2 contains all elements necessary for activation and emission of high-energy photons. It also simulates the chemical composition of explosives. The urea standard was put into an aluminum cylinder with a total weight of approximately 200 g and other urea standard was put into a steel bucket with total weight of approximately 5 kg. The size of the standard plays a small role in the measurement, as a bigger standard provides a larger amount of gamma-rays, but it also leads to a higher detector dead-time. The material of the container in which the urea standard is put is thin, so it does not shield the standard and thus the urea standard can be bombarded with neutrons without moderating them.

7.4   Setup and Configuration

Three measurements in two different laboratories were performed due to technical difficulties we met during measurements. The first and third measurement took place in a laboratory at VSB – Technical University of Ostrava. A room where the neutron activation was done is shielded by concrete walls and separated from the operation room to reduce the risk of exposure to radiation. The neutron generator is additionally shielded by high-density iron bricks to collimate the neutron yield into a beam directed towards the urea standard, which is placed between the neutron generator and spectrometer. The setup is shown in Figure 7.3 and Figure 7.4:

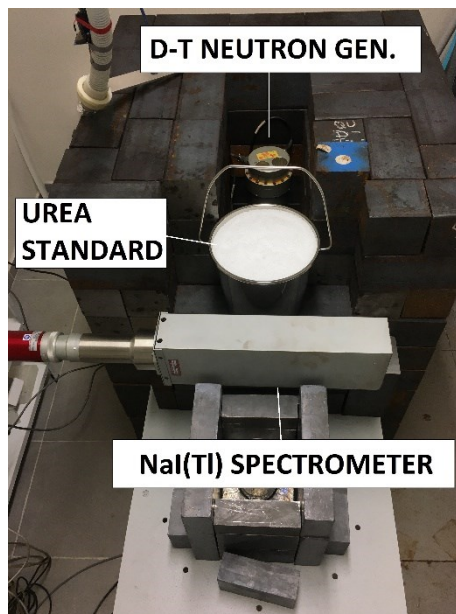Figure 7.3: Complete apparatus for the first and third measurement.

Figure 7.4: Placement of used components at VŠB-TU Ostrava.

The second measurement was carried out at the Department of Nuclear Reactors in Prague, where the training reactor VR-1 is situated. In this setup, the neutron generator was not collimated and neutrons were emitted in all directions, but because the measurement took place in a small-sized concrete chamber under the training reactor to sustain the best shielding capability, it can be considered as a collimated neutron beam. Additionally, the spectrometer was shielded by a small lead barrier. The urea standard was then placed on top of the spectrometer which was placed a small distance from the neutron generator. The setup is shown in Figure 7.5.

Figure 7.5: Placement of components at Department of Nuclear Reactors in Prague.

In both cases the configuration was the same. The spectrometer was connected to the computer via the ethernet cable and via the GPIO cable to the control unit of the neutron generator. A simple diagram in Figure 7.6 depicts the whole setup and how components are connected to each other. The GPIO cable is connected to the DELAY output, which allows the neutron generator to control the data acquisition of the spectrometer (see Section 8.1).
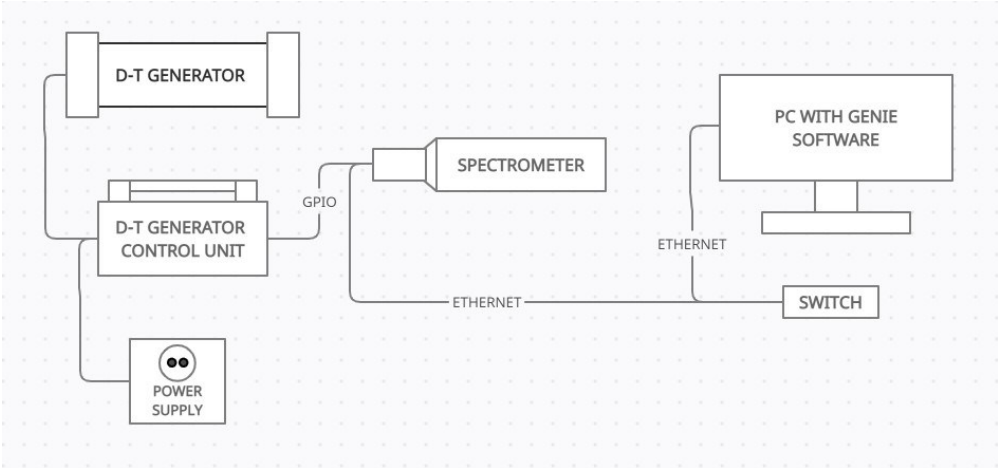

Figure 7.6: Overall arrangement of used components and their interconnection.

8.   Calibration of the NaI(Tl) Spectrometer

Total of 36 individual measurements have been carried out to gather spectra suitable for calibration. From all of these measurements only 7 have contained adequate data and visible peaks. With the intention of calibrating the NaI(Tl) Spectrometer on higher energy levels so the detector is able to detect activated elements, a series of more and more accurate calibrations ascending from lower energy range to higher energy range had to be performed, otherwise energy calibration would not be so effective. If we were about to perform a single energy calibration on one spectrum, the regression analysis would result in an inaccurate regression function and energy peaks would be assigned to different channels than they should be. As we will see, a few of these spectra have brought more problems than solutions and they are described at the end of this chapter.

8.1   Setup of the Genie 2000 Software and the NG Control Software

In Genie 2000 software the acquisition setup can be changed. When the acquisition is set to PHA+ mode (Pulse Height Analysis), an option of Start/Stop external control is available. The settings were constant and same for both measurements:
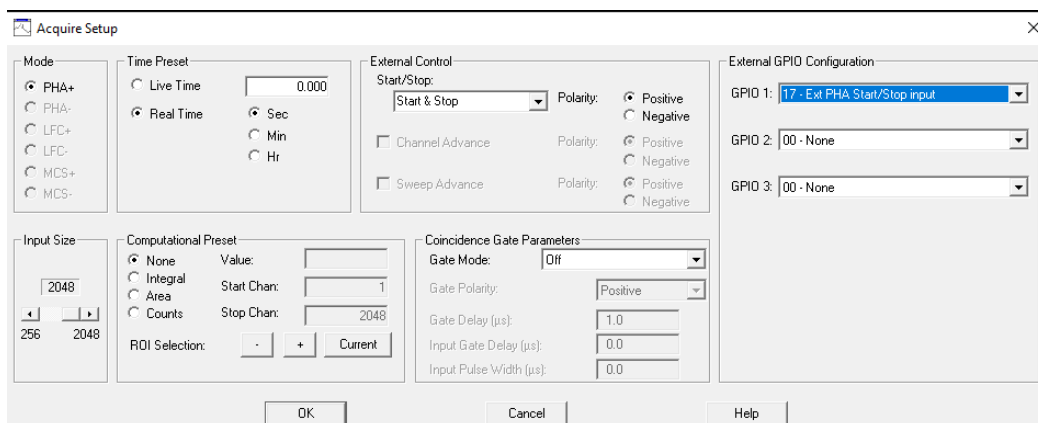

Figure 8.1: The setup of the Genie 2000 Software.

External Control was set to Suspend/Resume, so the spectrometer is controlled by incoming pulses from the neutron generator. If it was set to Start/Stop, the spectrometer would only measure one incoming pulse. External GPIO Configuration was set to a mode called "17 – PHA Ext. Output Signal" so the spectrometer is controlled by signals coming directly from the neutron generator.

In the software for the control of the neutron generator are pulse settings. In Figure 8.2 we can see that we are able to change the settings of the pulse width, delay time and also the frequency and duty factor (DF) of the pulses. If the duty factor is set to 100%, neutrons are emitted continuously, otherwise the percentage signifies the positive signal portion of the one pulse. Correct combinations of these settings are required in order to achieve good results and even a little change significantly affects the whole measurement.
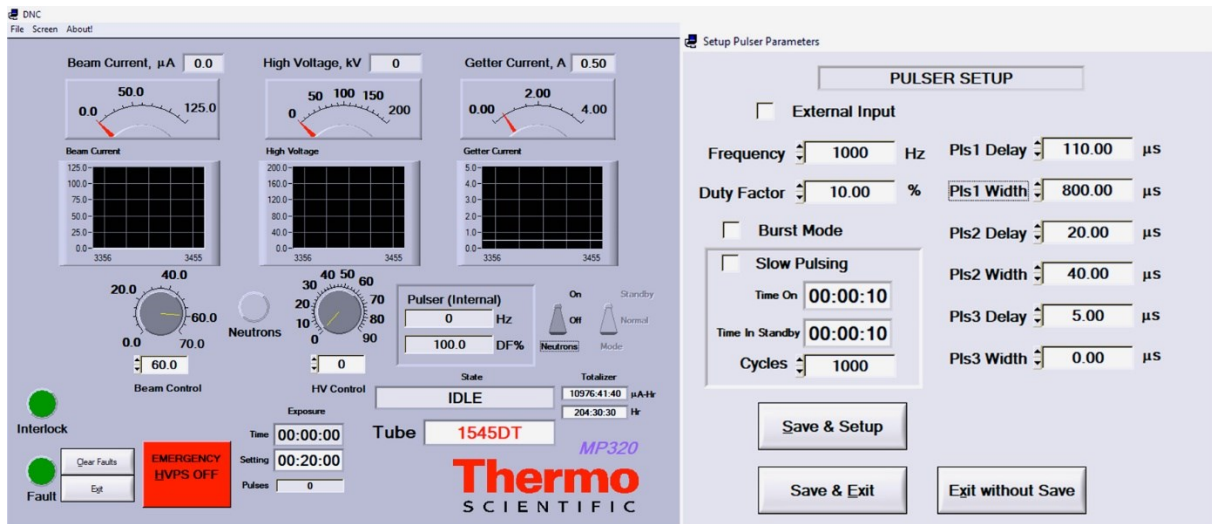
Figure 8.2: Left window is the control software of the NG; In the right window are the pulse settings.

A technical issue in the Genie 2000 software caused a wrong processing of the output signal from the NG. The polarity of the output signal was positive and at the beginning of the pulse it should have started the acquisition and at the end of the pulse it should have suspended the acquisition, but the technical issue considered the signal as if it had a negative polarity, therefore the acquisition started when the incoming pulse was detected and paused, when the signal that the NG is emitting neutrons disappeared. In short, the detector confused the polarity of the output signal from the NG and started the acquisition when it should not have. To fix this issue, we had to delay the output signal and by that create a "fake" or "ghost" signal to trick the detector. The NG then outputs a signal with a delay, the detector captures the signal, but in reality it was the "ghost" signal and the real pulse was delayed in time, resulting in a correct polarity of the signal. This was achieved by a simple calculation and correct setup of the NG pulses and delay times, where the delay time and width is calculated with respect to the frequency and duty factor. Figure 8.3 depicts the principle with these calculations included.
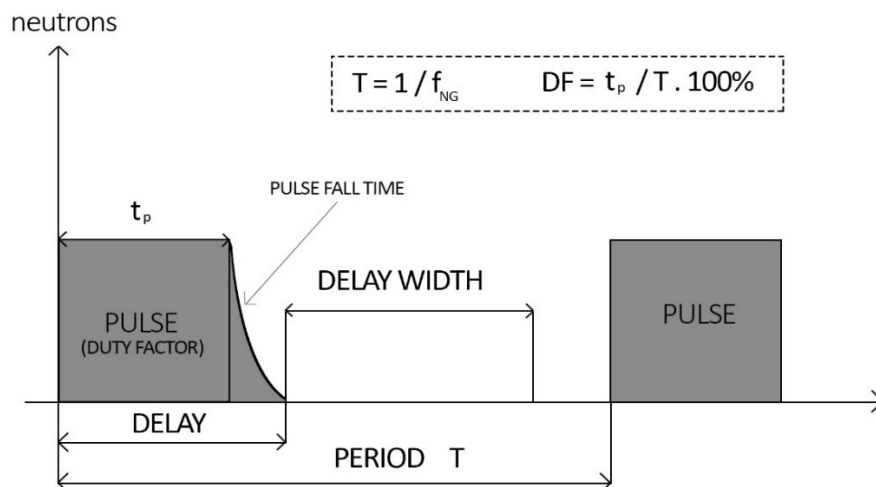

Figure 8.3: A graphical explanation of the delay time, delay width and duty factor.

8.2   Spectra Used for Calibration

Spectra that have been used for calibration were gathered both at the Department of Nuclear Reactors in Prague and mainly at VŠB – TU Ostrava. For the series of calibration we have used standards emitting gamma-rays of energies below 2,6 MeV level and gradually worked our way up to 7,6 MeV from neutrons activated Fe. Spectra themselves were taken from the Genie 2000 software, because they are more simple to interact with and overall it is more convenient than exporting the data to other software. A major issue occurred when trying to compile multiple calibrations together. Instead of using the "Append to existing calibration" option, I had to create a calibration file for each measurement and load it before the calibration on the next spectrum, because the software could not load calibrations on entries of energy values written by myself and therefore it could not continue in previous calibration.

8.2.1   Cesium-137 and Cobalt-60 Standards

A combination of these two standards were used for the initial and essential calibration. Both of these isotopes have distinct energy peaks in lower range and due to their significance in a spectrum they cannot be misinterpreted with other peaks. Figure 8.4 shows the measured spectrum and as we can see - four distinct peaks are visible. By using a function "Energy Calibration by Nuclide List" we are able to manually select the peak and assign it to the correct energy value given by a nuclide library within the software. After the selection of a channel at the top of each peak the Table 8.1 (data from Genie 2000 nuclide library) was compiled and the energy value shown in the software at the given channel is compared to actual and correct energy value.

Element	Channel	Software Energy Value (keV)	Correct Energy Value (keV)
Cs-137	111	660,9	661,657
Co-60	193	1164,6	1173,2
Co-60	218	1318,2	1332,49
Co-60 sum peak	410	2498,8	2505,69

Table 8.1: Cs-137 and Co-60 and their energies at according channel

A sum-peak of Co-60 is nicely visible at the end of the zoomed energy range. Unfortunately, another error in Genie 2000 software occurred repeatedly disallowing me from choosing the Co-60 1173,2 keV peak for calibration, therefore it was deleted from the calibration file. If two differents peaks were close to each other, the software considered them as a one single wide peak and assigned the gamma energies to a single channel, resulting in an error in the calibration function.
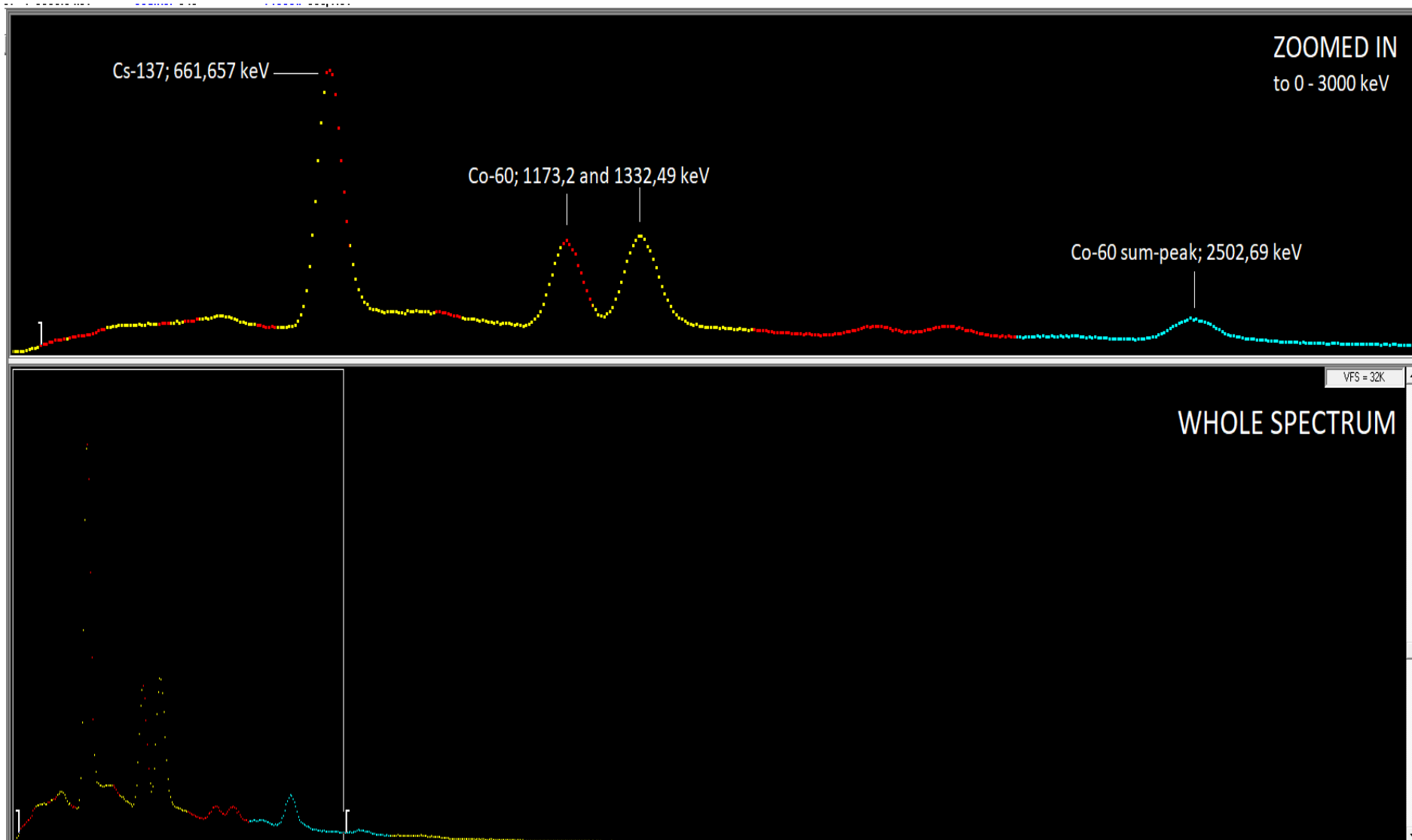
Figure 8.4: The spectrum of Cs-137 and Co-60 standards.

8.2.2 Thorium-232 Standard

The next energy calibration was performed using Th-232 standard with energies again in the lower range, but in the Figure 8.5 we can see that no major peaks appear. Only two Th-232 peaks were used for calibration, again due to the error in Genie 2000 software, but also because their significance in calibration in the higher energy range is minimal. Peaks from the Th-232 decay chain also appear in other upcoming spectra, but they are not added to calibration files anymore. Additionally, the K-40 peak is perfectly visible and its energy value was included in the nuclide library, thus it was also added to the calibration file. The Figure 8.2 also shows U-238 and Th-232 decay chain products gamma energy peaks, but in order to make the calibration as accurate as it can get, the U-238 decay chain energy peak and Th-232 decay chain energy peak were excluded from the calibration due to their shape and inconsistency. In the lower part of Figure 8.5 where the whole spectrum is shown the Th-234 is marked. The Th-234 isotope is also a product of U-238 decay chain and its gamma-rays have an energy of approximately 63 keV, but again, such a low energy value is not important for us (data from [37]).

Element	Channel	Software Energy Value (keV)	Correct Energy Value (keV)
Th-232	100	593,3	583
K-40	242	1465,7	1460,8
Th-232	426	2596,2	2614

Table 8.2: Th-232 and K-40 and their energies at according channels.

In the Table 8.2 there are notable differences between the energy values determined by the software and the actual energy value of the respective gamma-ray, indicating the calibration at lower energy levels was somewhat accurate, but the 2,614 MeV peak was quite shifted from the software value. This is leading us to the third calibration.
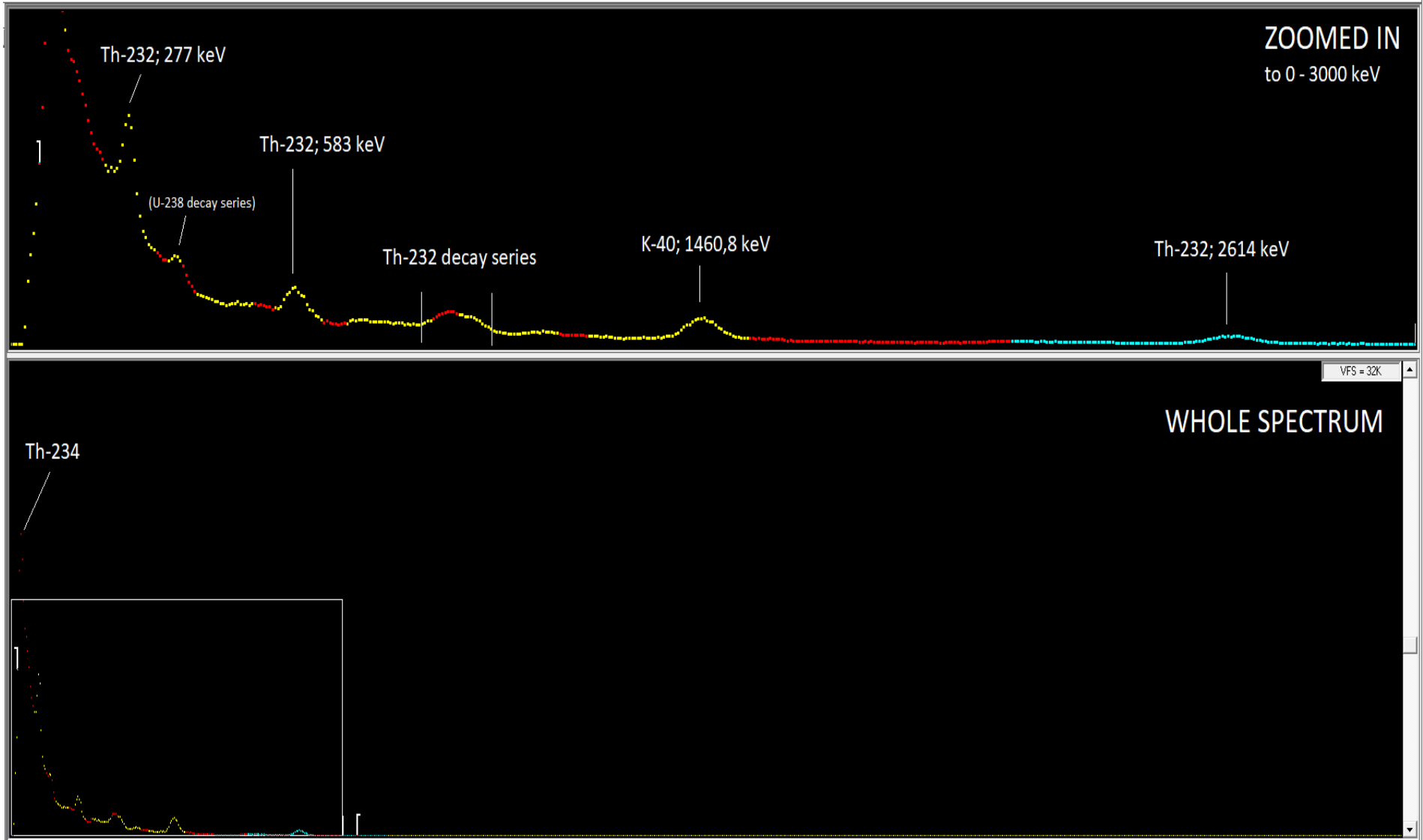
Figure 8.5: The spectrum of K-40 and Th-232 standards.

8.2.3 Europium-152 Standard

In previous calibration we could note that the energy values were still a little bit shifted from the actual energy values of the gamma-rays. To prevent us from further errors in calibration, a standard containing the Eu-152, that is usually used for multi-peak calibration, was used. Briefly, the objective of this calibration is to make the energy calibration more precise in lower energy range to find energy peaks with corresponding energy easily in gradually higher energy levels. By adding multiple peaks to the calibration file the regression analysis gets more accurate. Table 8.3 (data from Genie 2000 nuclide library) lists Eu-152 gamma-rays energies used for calibration from which some of them were once again deleted due to the mentioned error in the software.

Element	Channel	Software Energy Value (keV)	Correct Energy Value (keV)
Eu-152	23	116,5	121,78
Eu-152	*43*	*240,2*	*244,69*
Eu-152	60	345,3	344,27
Eu-152	*132*	*790,4*	*778,89*
Eu-152	*162*	*975,9*	*964,01*
Eu-152	186	1124,2	1112,02
Eu-152	235	1427,2	1407,95

Table 8.3: Eu-152 and their energies at according channels; italic font symbolises those energy levels that were not used for the calibration.

In Figure 8.6 the Eu-152 peaks are very prominent and the precise choice of a channel on the top of the peak was a matter of zooming in on the peak and a simple cursor click. Once again the energies of Eu-152 are listed in Genie 2000 nuclide library within the software so the function "Energy Calibration by Nuclide List" was used again. This function also has an option "Append to existing calibration" and thus we did not have to save the calibration as a separate file, because the calibration was added to the previous calibration file performed on the Th-232 standard, but to make sure that we do not lose this data, I continued to save the calibration as a separate file and loaded it up before performing next calibration. This method also serves as a "checkpoint" – if we load the calibration file, we can check how the calibration changed compared to previous calibrations and if it got any better. The following calibration was performed to verify the theory.
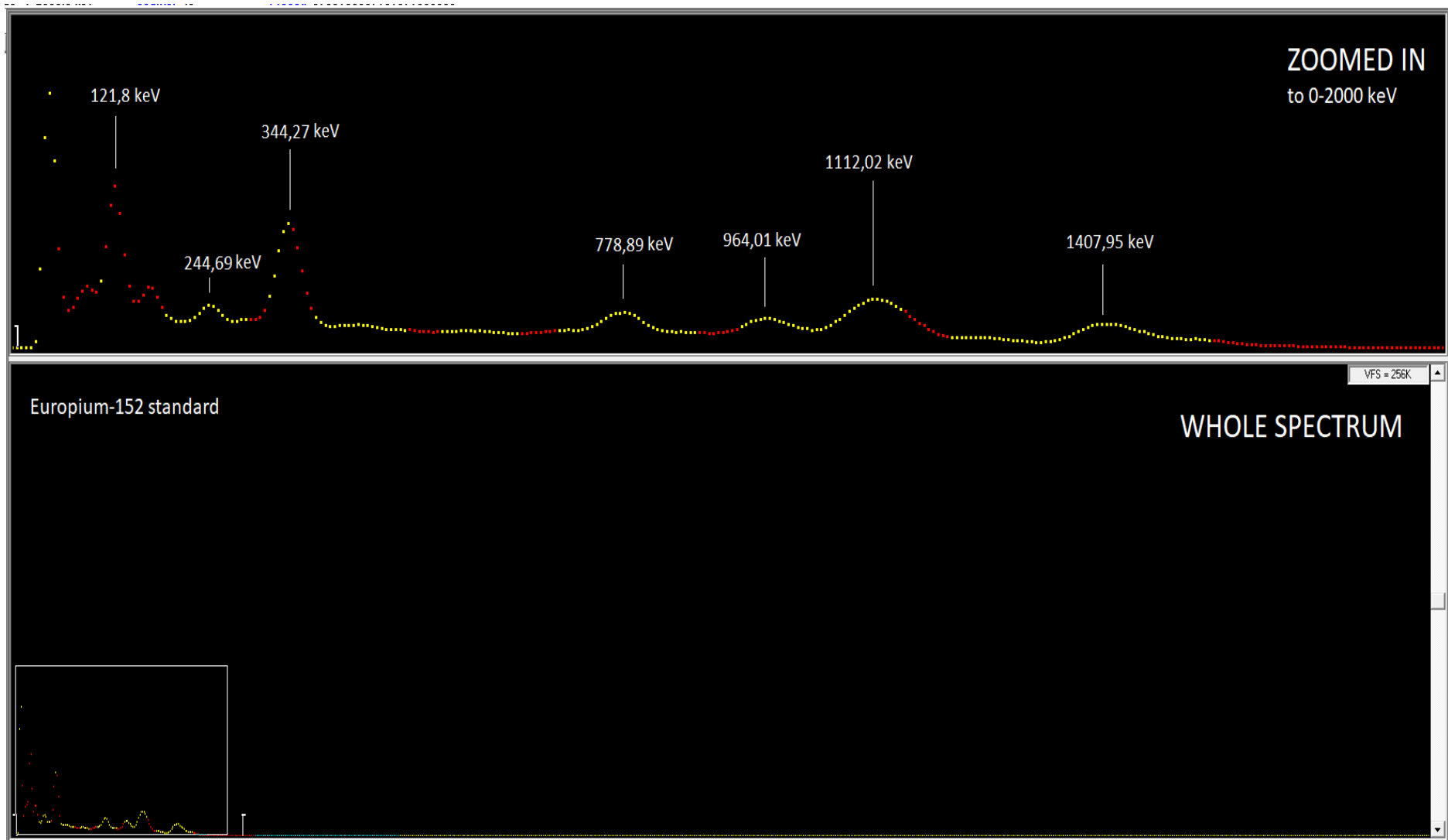
Figure 8.6: The spectrum of Eu-152 standard.

8.2.4 Hydrogen Activated by Thermal Neutrons

This measurement took place at the Department of Nuclear Reactors in Prague where we had an opportunity to also test out the D-D Neutron Generator that produces slow/thermal neutrons from the Deuterium + Deuterium fusion. Hydrogen then captures a neutron (is activated) and decays with emission of photons with energies of 2,22 MeV [33]. With this photon energy value and significant energy peak in the spectrum the calibration on activated hydrogen represents a middle point between low energy range and a higher energy range and is a gate to further calibrations. Calibration on this single peak improves the regression analysis and because the hydrogen peak appears in every single spectrum with neutron activated carbon, oxygen and nitrogen, it also serves as verifier if the calibration is still correct in upcoming spectra. Table 8.4 (data from [33]) shows that the peak is slightly shifted from the correct position.

Element	Channel	Software Energy Value (keV)	Correct Energy Value (keV
H	360	2199,1	2223,2

Table 8.4: Photon energy of activated H used for the calibration.

In the previous section I have mentioned that we could use the calibration files to check how the calibration shifted in comparison with the previous calibration. In this spectrum, the energy at channel 360 (before loading the calibration file from the Eu-152 spectrum) was 2181,1 keV. In the Table 8.4 is obvious the improvement of the calibration, but still we can see some shift.

In the vicinity of the hydrogen peak in Figure 8.7 a significant increase in counts is visible. This could be reasoned by the activation of other elements in materials surrounding the D-D generator and the NaI(Tl) spectrometer. The D-D generator was put into polyethylene blocks and the detector was placed right next to the generator with shielding. Another clue was also that the deadtime of the detector reached up to 50%, implying that the number of counts it detected was enormous and probably came from the activated materials, because no other radioactive materials were nowhere near it.

From now on, the energies of activated materials are not listed in the nuclide library within the Genie 2000 software and the calibration had to be performed using a function "Energy Calibration by Entry". There was no major difference between this function and the function "Energy Calibration by Nuclide List" in principle, except that I had to type in every energy value myself and assign it to a channel using a cursor. An unexpected issue occurred when I was about to use the option "Append to Existing Calibration" – the option was not there anymore. Fortunately, I continued saving the calibration in a separate file, which turned out to be a better way of saving the calibration onto the next spectrum.
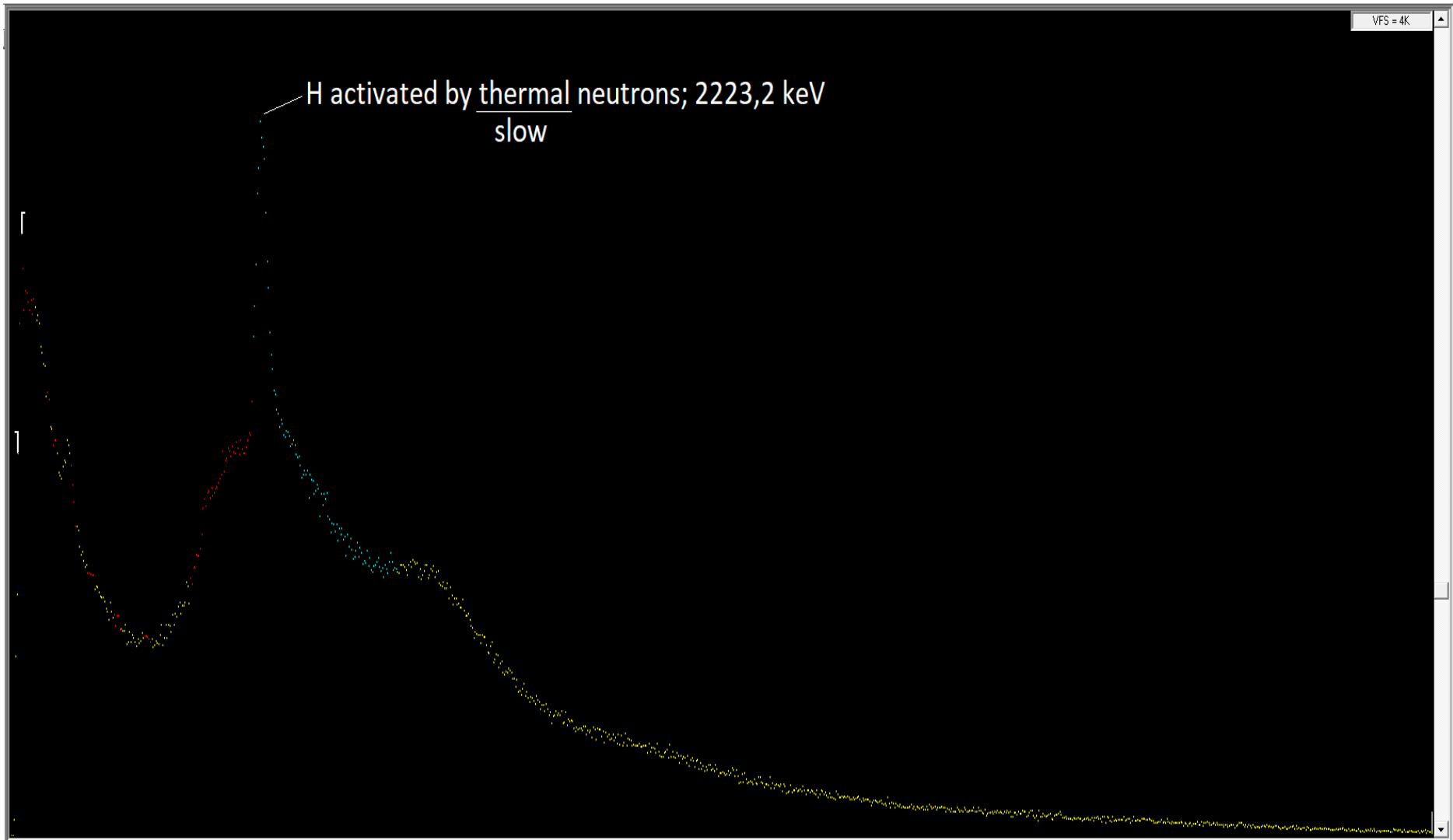
Figure 8.7: The spectrum of Hydrogen activated by neutrons.

8.2.5 Polyethylene Activated by 14 MeV Neutrons

Back at the laboratory at VŠB – TUO, we performed a measurement where we put a block of polyethylene $(C_2H_4)_n$ between the D-T Neutron Generator and detector. We expected to measure only the energy of photons produced from decay of activated hydrogen and carbon, which is the first neutron activated element with photon energy higher than 3 MeV, but we have measured something unexpected as well. Figure 8.8 shows the placement of components used in this measurement.

Figure 8.8: The placement of polyethylene blocks.

The neutron generator was surrounded by both polyethylene blocks and high-density iron blocks. Because of this, 14 MeV neutrons activated iron blocks as well and distinct Fe-56 energy peaks are visible in Figure 8.9. The spectrum is viewed in logarithmic scale to improve the visibility of each peak. If we used the linear scale, the peaks would not be so distinct. Because these energies appear both in lower energy range and higher energy range, they were also included in the overall calibration. In the following sections where the calibration was performed and improved on a spectrum that was measured in Prague, we can notice that Fe-56 energy peaks disappeared in Figure 8.10, because there was no iron shielding in that laboratory. The Table 8.5 (data from [22-33]) again lists channels and energies used for the continuous calibration and added to the complete calibration file, a notable improvement in accuracy of the calibration can be seen.

Element	Channel	Software Energy Value (keV)	Correct Energy Value (keV)
Fe-56 (act)	143	857,4	845,76
Fe-56 (act)	205	1241,1	1238,3
H activated	364	2225,1	2223,2
C activated	724	4453,0	4439,0
Fe-56 (act)	1232	7596,9	7631

Table 8.5: Activated Fe-56, activated H and C and their energies at according channels.
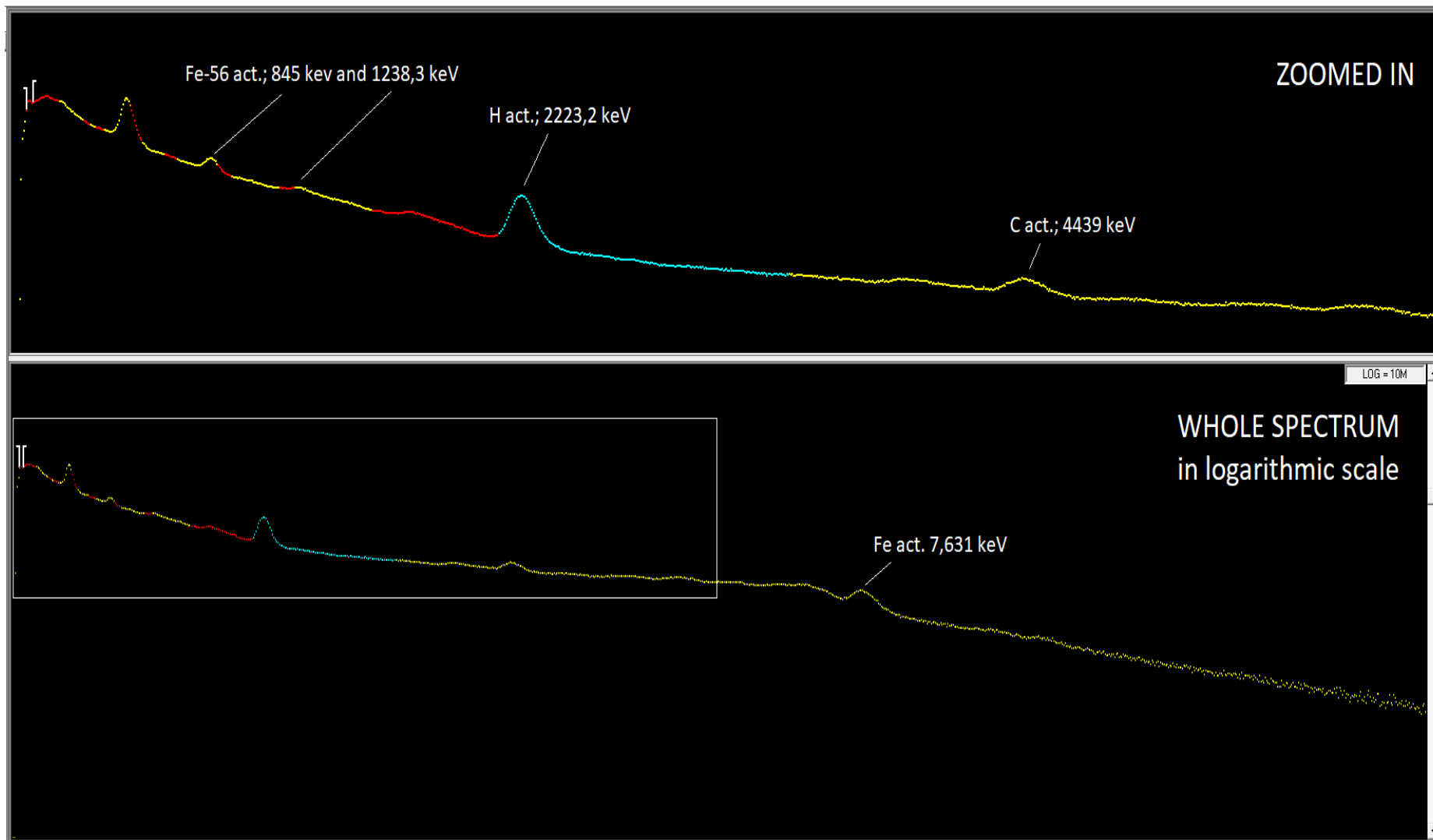
Figure 8.9: The spectrum of polyethylene activated by neutrons.

8.2.6 Pulse Activation of the Urea Standard – Spectrum 1

Data for this spectrum was obtained in Prague. A step towards the calibration in higher energy range was made in previous calibration, thus using the same D-T Neutron Generator (MP320) as we have at our laboratory in Ostrava, we were able to set up the pulse activation of the urea standard, which would (by our expectations) emit photons with energies up to 10 MeV. The generator used in Prague was almost the same as ours in Ostrava, therefore the results should be the same. The overall setup and configuration was described in the Section 7.4 and problems with the output signals from the NG were described in Section 8.1. As a result, the configuration of the NG pulses summarized in Table 8.6 was used.

Pulse Frequency	200 Hz
Duty Factor	10%
Pulse Delay	500 μs
Delayed Pulse Width	4000 μs

Table 8.6: The first configuration of the NG pulses.

When the spectrum was viewed in linear scale, no distinct peaks could be seen at the first glance, but when we switched to logarithmic scale a lot of them appeared. In Table 8.7 (data from [22-33]) are listed gamma energies of activated elements at higher energy levels that we haven't seen before. For the calibration we used only the recognizable ones from Figure 8.10.

Element	Channel	Software Energy Value (keV)	Correct Energy Value (keV)
H activated	362	2223,0	2223,2
O activated	573	3513	3684
N activated	794	4911,6	4951
O activated	1027	6262,2	6129,9
O activated	1098	6756,4	6917,2

Table 8.7: Activated H, O and N and their energies at the according channel.

Let me note a few observations from Table 8.7. First, we can see how the previous calibration on polyethylene was precise, because the gamma energy of activated hydrogen is almost the same as the correct one. Second, for other elements the calibration shifted, but we were counting on it, because this is the initial calibration in this energy range. The last thing we can notice is that no Fe-56 energies were measured, because there was no iron shielding used in Prague.

The allocation of the peaks was again only a matter of zooming in and using the interactive environment within the software. After the calibration on this spectrum, we are prepared to do the final step and complete the overall calibration.
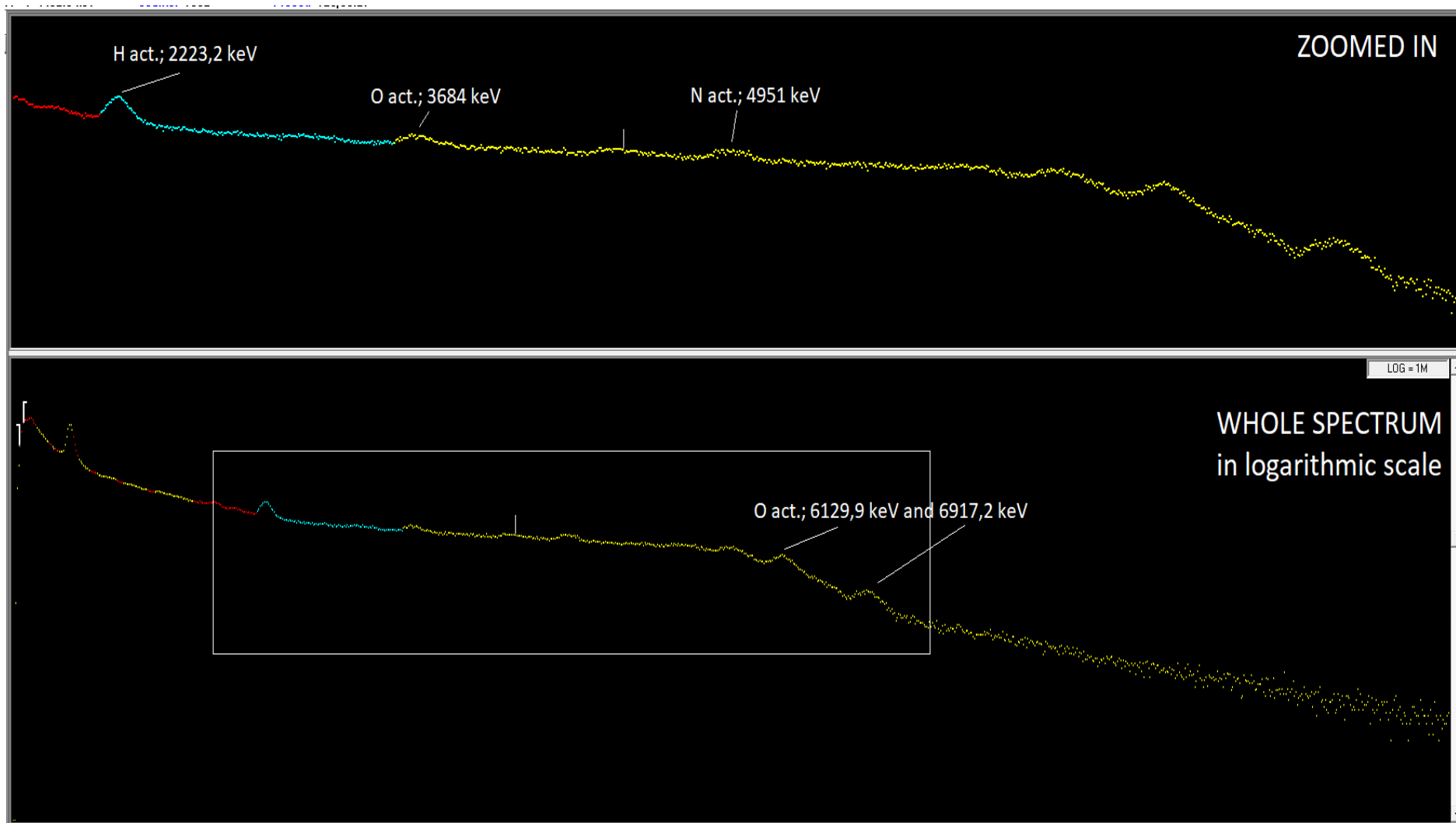
Figure 8.10: The first spectrum of activated urea standard.

8.2.7 Pulse Activation of the Urea Standard – Spectrum 2

The complete and final calibration was carried out on a spectrum that was measured in our laboratory at Ostrava. After learning how to configure the neutron generator and what to pay attention to so the obtained data are the best, we were able to gather many more gamma energies and peaks for the calibration than on the previous measurement. Different configuration of the neutron generator was used as shown in Table 8.8.

Pulse Frequency	1000 Hz
Duty Factor	10%
Pulse Delay	110 µs
Delayed Pulse Width	800 µs

Table 8.8: The second configuration of the NG pulses.

Once again the neutron generator was in an iron shielding, which resulted in activation of Fe, but also it collimated the neutron source into the urea standard and the neutron activation improved. In Table 8.9 (data from [22-33]) are listed those gamma energies gathered from distinct peaks in the spectrum shown in Figure 8.12.

Element	Channel	Software Energy Value (keV)	Correct Energy Value (keV
H activated	365	2232,0	2223,2
O activated	577	3544,4	3684,4
C activated	717	4411,1	4439,0
N activated	802	4937,3	4915,0
O activated	968	5964,9	6130
N activated	1032	6361,1	6446,2
O activated	1111	6850,1	6917,1
Fe-56	1231	7593,0	7631
Fe-54	1493	9260,9	9297,9

Table 8.9: Activated Fe, H, C, N and O and their energies at according channels.

Major deviations in energy values can be seen. They are probably a result of the calculations within the Genie2000 software that tries to correlate the peak width and channel together for a better calibration. Also the reason can be the fact that the previous calibration was performed on less data than we have gathered in this spectrum and therefore the previous calibration was not so effective and precise. But finally we were able to reach the highest energy value in all of our meaurements – the Fe-54 9,3 MeV energy. The Figure 8.11 on the following page is a zoomed-in view at the peak of Fe-54 in the range of 8000 to 10000 keV.
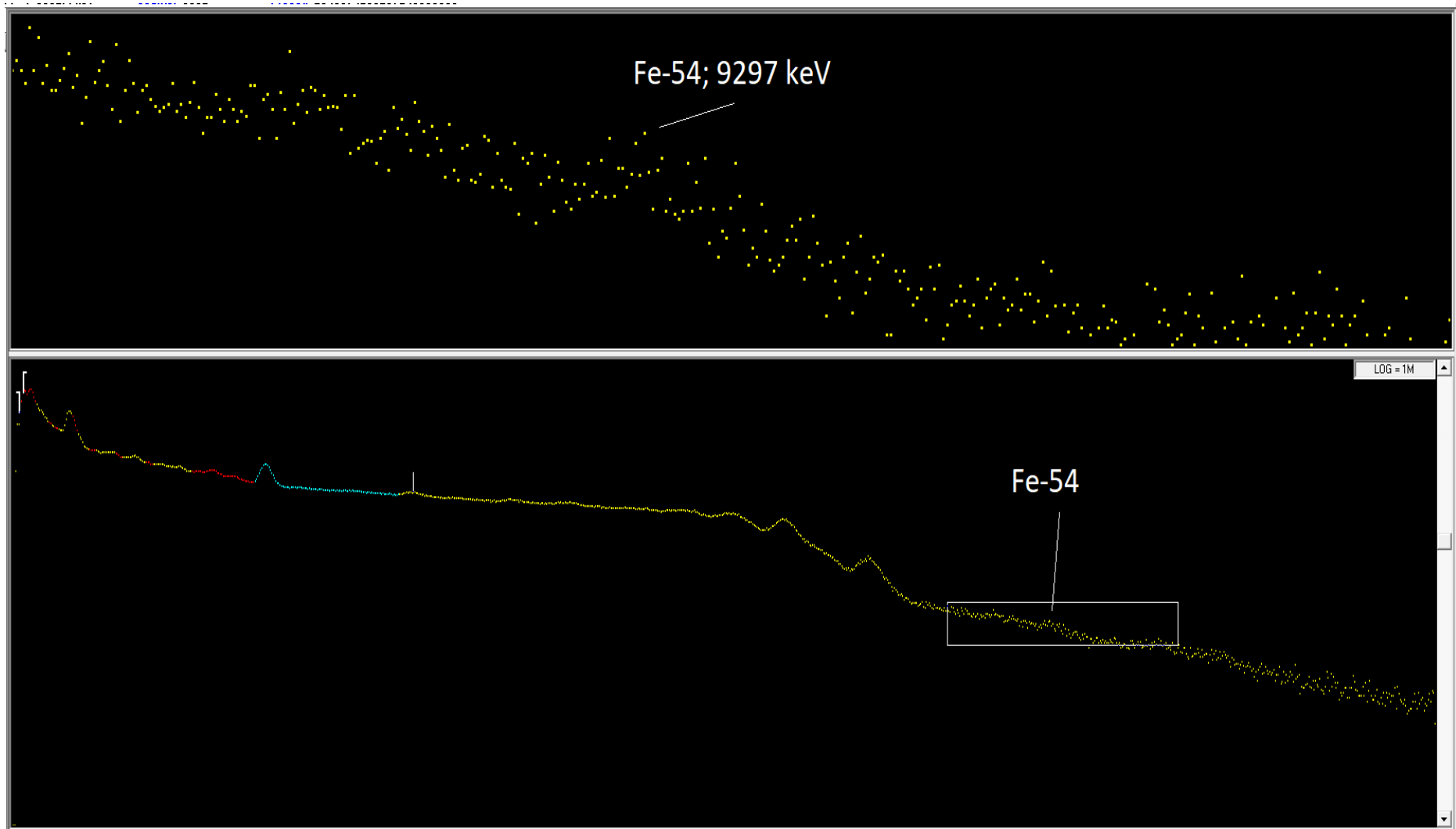
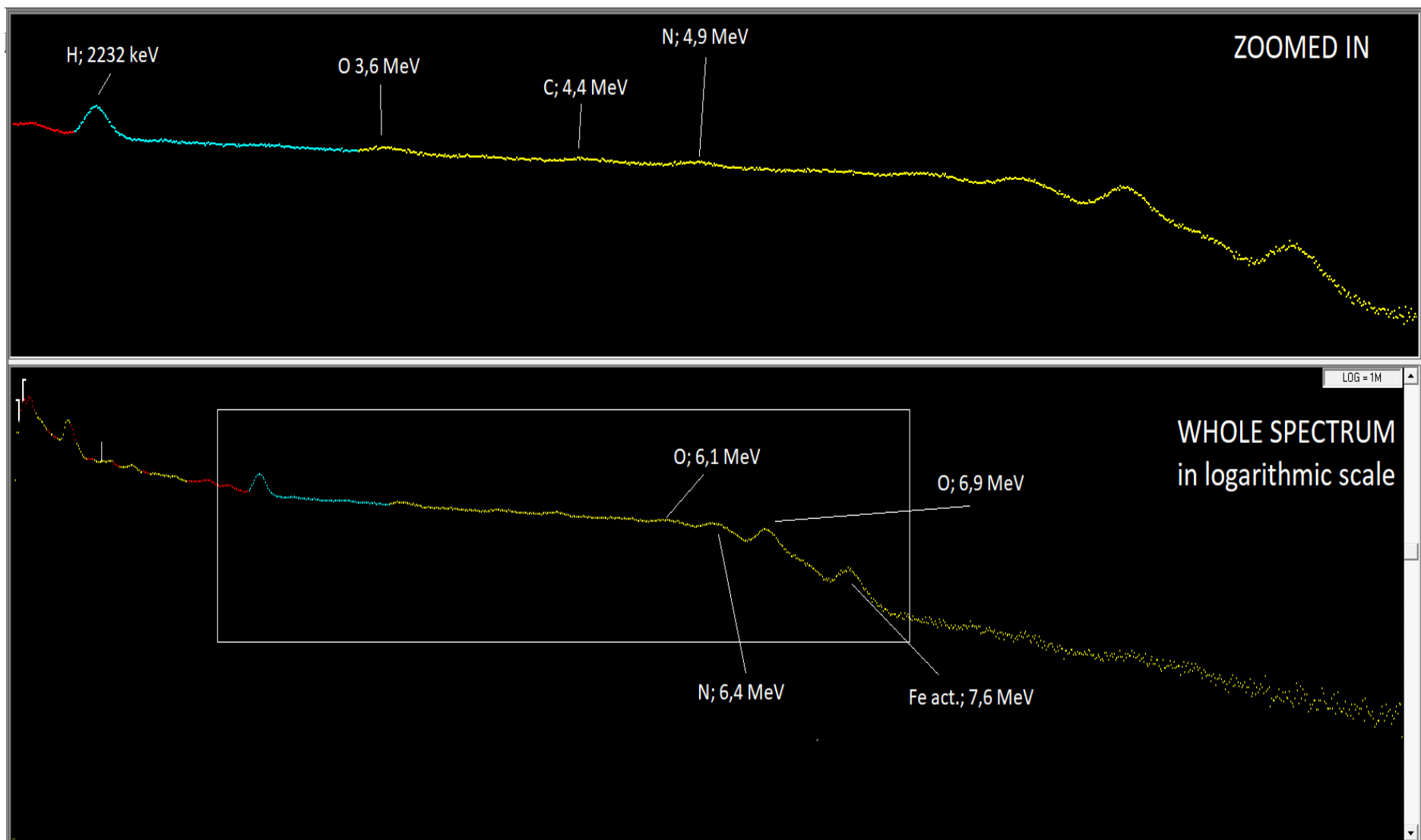Figure 8.11: Zoomed-in view at the peak 9,3 MeV peak of Fe-54.

Figure 8.12: The second spectrum of activated urea standard.

8.3 Complete Calibration

Now the series of calibrations is complete and the detector can be considered as calibrated on higher energy levels. All of the gamma energies used for the overall calibration were exported from the final calibration file and are listed in the Table 8.10 (data from [22-33]) also with the channel error of the calibration.

Element	Channel	Channel Error (±)	Correct Energy Value (keV)
Eu-152	22,98	0,16	121,78
Eu-152	60,15	0,03	344,27
Th-232	101,31	1	583
Cs-137	111,13	0,05	661,66
Eu-152	185,87	0,43	1112,02
Fe-56	213,25	1	1238,3
Co-60	218,92	0,68	1332,49
Eu-152	238	0,47	1407,95
K-40	241,78	0,22	1460,8
H act.	364,88	0,18	2223,2
Co-60 sum-peak	411,32	0,23	2505,69
Th-232	426,05	0,14	2614
O act.	572,4	0,51	3684
C act.	716,08	0,16	4439
N act.	803,57	0,08	4915
O act.	968	0	6130
N act.	1045,51	0,12	6446,2
O act.	1112,63	0,18	6917,1
Fe-56	1232,21	0,41	7631
Fe-54	1493,18	0,67	9297,9

Table 8.10: All of the elements used for the complete calibration.

The value (or a number) of the channel assigned to the energy was determined by the Genie 2000 software itself and by calculations within the "Energy Calibration by Entry" function. Once we have all of the channel numbers, and required energy assigned to them, we are able to compile a regression function of the calibration. This was also done using the Genie 2000, but to precisely show the points from which the regression has been compiled from, the Figure 8.13 was created in Microsoft Excel program. The energy calibration in general is expressed in Eq. 4.1:

$$E(keV) = I(keV) + G \times C(channel), \tag{4.1}$$

and by calculations for the calibration file the energy calibration is:

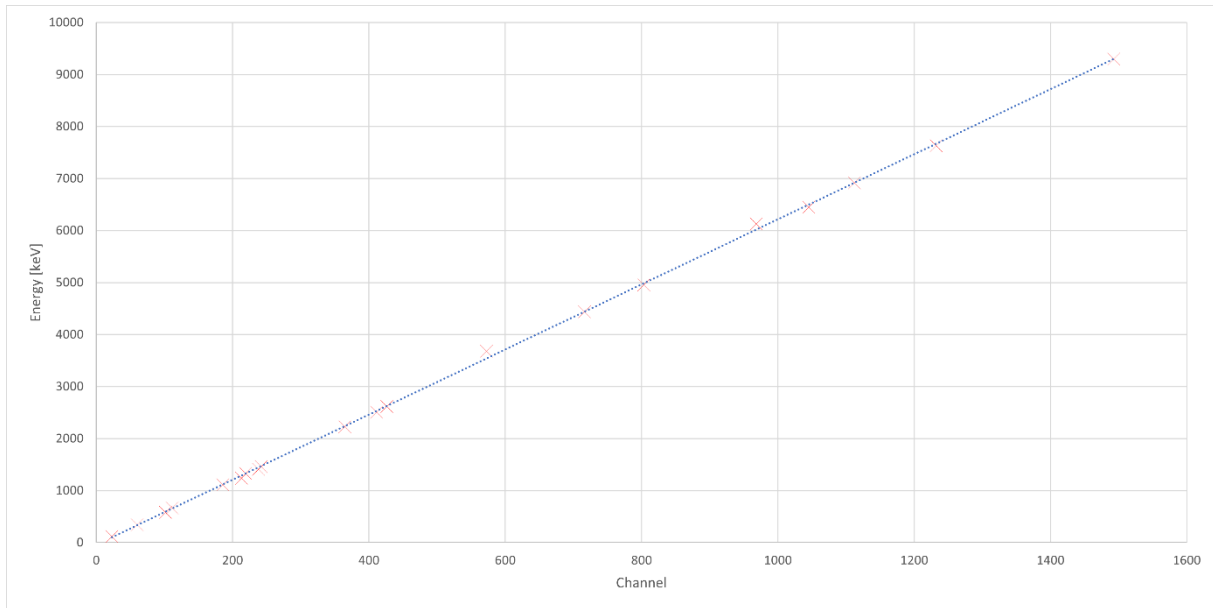$$E(keV) = -30{,}97 + 6{,}228 \times C(channel). \tag{6.1}$$

Figure 8.13: The energy calibration plot.

To verify that the calibration is correct and complete, we loaded the calibration file into a datasource with a different spectrum that we have not used yet. The spectrum looked very similar to the one in Figure 8.12, therefore we may expect the same peaks as in Table 8.9, but with correct energy values at according channel. To do so, we exploit an analysis algorithm called "Peak Analysis w/Report", that goes through the whole spectrum, finds peaks and assigns energies to those peaks. This algorithm was not used for the calibration itself, one may think it would save us some time and make the search of the peaks easier, but since the peaks appearing in the spectrum are small compared to the peaks of eg. Cs-137 or Co-60, we should not rely on this function. The peak analysis came up with results listed in Table 8.11 (data from [22-33]). The error δ_r expresed in percentage indicates how different the energy given by the software is from the corrent energy value.

Element	Channel	Software En. Value (keV)	Correct En. Value (keV)	δ_r (%)
K-40 (bg.)	240,9	1469,24	1460,1	0,63
H act.	365,32	2244	2223,2	0,94
O act.	575,69	3554,06	3684,4	-3,54
C act.	719,26	4448,1	4439	0,21
N act.	801,53	4960,42	4915,1	0,92
O act.	978,84	6064,53	6129,9	-1,07
N act.	1037,35	6428,9	6446,2	-0,27
O act.	1112,04	6894,02	6917,1	-0,33
Fe-56	1233,04	7647,52	7631	0,22
Fe-54	1416,04	8787,1	8870,3	-0,94
Fe-54	1492,06	9260,48	9297,9	-0,40

Table 8.11: Energy values determined by the Peak Analysis w/Report compared to actual energy values of the radionuclides.

Gamma energies determined by the Peak Analysis algorithm are very close to the actual gamma energy values of activated elements. The algorithm also surprised us with finding the additional two peaks of the isotope Fe-54 which are a result of iron being activated by 14 MeV neutrons. Peaks are not quite visible in the spectrum itself, but by using a mathematical approach (Gaussian regression and interpolation) it was capable of finding them. Other datasources were also calibrated using our calibration file and came up with similar and accurate results. We could continue in analysing the spectra that we have measured, but because they all look the same (eg. see Section 8.3.3) I would rather discuss the issues with the calibration.

8.4   Issues with Calibration on NaI(Tl) Spectrometer

During the measurements we have encountered several issues and difficulties with the measurements themselves, and other, mainly technical matters. I will introduce some of them in order to better understand the limits of detection of gamma-rays with a NaI(Tl) spectrometer, to show what to pay attention to and so on.

8.4.1   Overall Calibration Issues

When one wants to calibrate the spectrometer in higher energy levels, he should think in advance of many aspects of the measurement. Data of gamma energies of activated materials vary from science articles to books to databases and it seems like that scientist have not agreed on a 100% exact gamma energy values of the activated elements yet. These deviations and differences are not that drastic, but even a 100 keV difference throughout several databases makes a tremendous effect on the energy calibration. There are several online databases and literatures focusing on this subjecting and trying to gather vast amount of data to create a stable value of the gamma energies, but considering the requirements and difficulty of both the neutron activation in its principle and the detection of the gamma-rays coming up from the activation, nobody can be ultimately sure that the apparatus used by them lead up to a correct value. This is also a matter of our calibration – I gathered gamma energies from various sources with the intention selecting those values, that the majority of experimentators have used, but we too cannot be so sure if these values are correct and should be used for calibration. Additionally, from these sources only those, where a measurement apparatus similar to ours is used, were chosen, so we are able to replicate those experiments and rely on the same energy values as they have achieved.

In the Section 4.5 was mentioned that except the energy calibration, detectors undergo an efficiency calibration as well. The **efficiency calibration** is done using standards with known activity of the radionuclides and with referential date, so the experimentator is able to calculate the activity of the standard in the actual time. When we measure the spectra of activated urea standard, no information about its activity, or the original number of photons emitted in the given time is provided. A complicated mathematical approach to this matter could lead us to an approximate number of photons, but since the number is estimated and not actual, the efficiency calibration is uneffective.

Another issue with the calibration is the unavailibility of performing a polynomial regression on gathered data in Table 8.9 within the detector software. Obviously, it can be done using different software than Genie 2000 and it would lead to better results, but the Genie 2000 does not have an

option that would allow us to use a polynomial calibration function or to include the polynomial calibration in the Genie 2000 software environment.

8.4.2   Activation of the Na within the Detector

A major disadvantage of the NaI(Tl) crystals is that the sodium within the detector crystal can be activated by slow, thermal and 14 MeV neutrons. The main reaction occuring inside is ^{23}Na(n,2n)^{22}Na with the emission of gamma-rays of 1274 keV and formation of annihilation peak with the energy of 511 keV [38]. The cross section of this reaction is quite small and insignificant for the measurements of activated H, C, N and O elements, but the fact that the activation of Na is still possible and could result in Na peak overlapping another peak of element in our interest or combining two peaks together (eg. the Co-60 has two major peaks at 1173 and 1332 keV, the Na peak at 1274 keV is right in the middle of them), it should be taken into consideration when choosing the detector for needed measurements. During a measurement with pulses set on a low frequency, the activation of Na was prominent as shown in Figure 8.14.
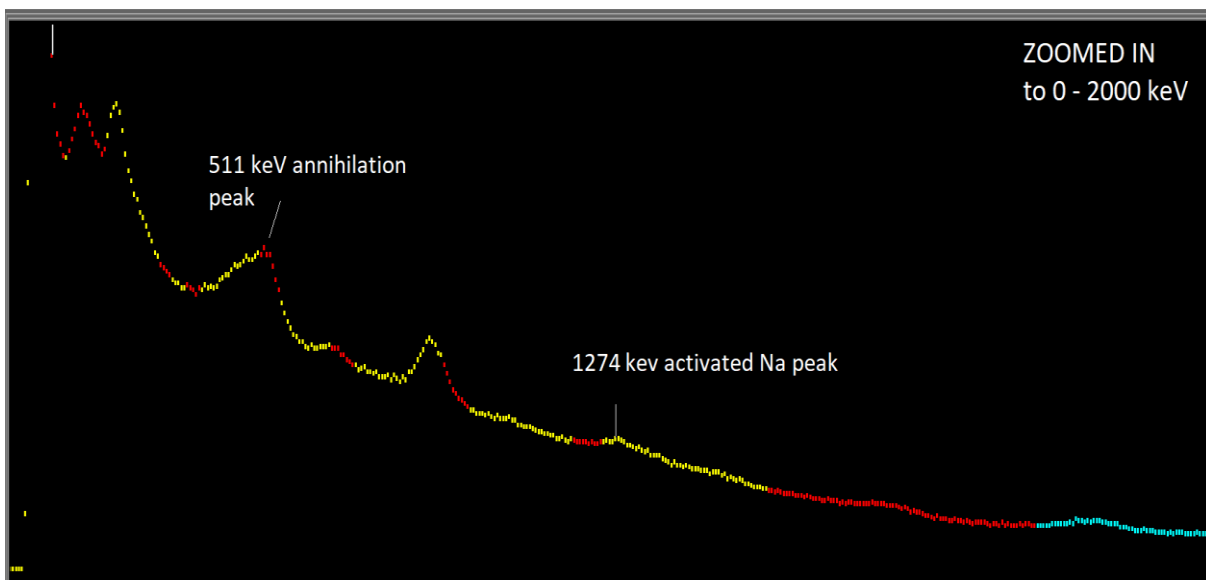

Figure 8.14: The activation of sodium within the detector (f = 500 Hz).

Also, considering the higher volume of the detector, the possibility of the activation of Na increases compared to casual 7" spectrometers. Fortunately, the effect of activated Na was minimal in other measurements.

8.4.3   Appropriate Configuration of Neutron Generator

Probably one of the most problematic aspects of our measurements was the appropriate configuration of the neutron generator and issues coming up with it. There are several values that can be changed and arranged so the acquisition of the data comes up better. An example of using a different configuration for each measurement is shown in Figure 8.15. Nine measurements in total were performed and all of them were measured with a real-time limit of 100 seconds, beam current set to 20 μA and voltage set to 60 kV. One of those spectra was also used for the calibration and can be seen in the Section 8.2.6, for which the configuration of the NG was the most suitable.
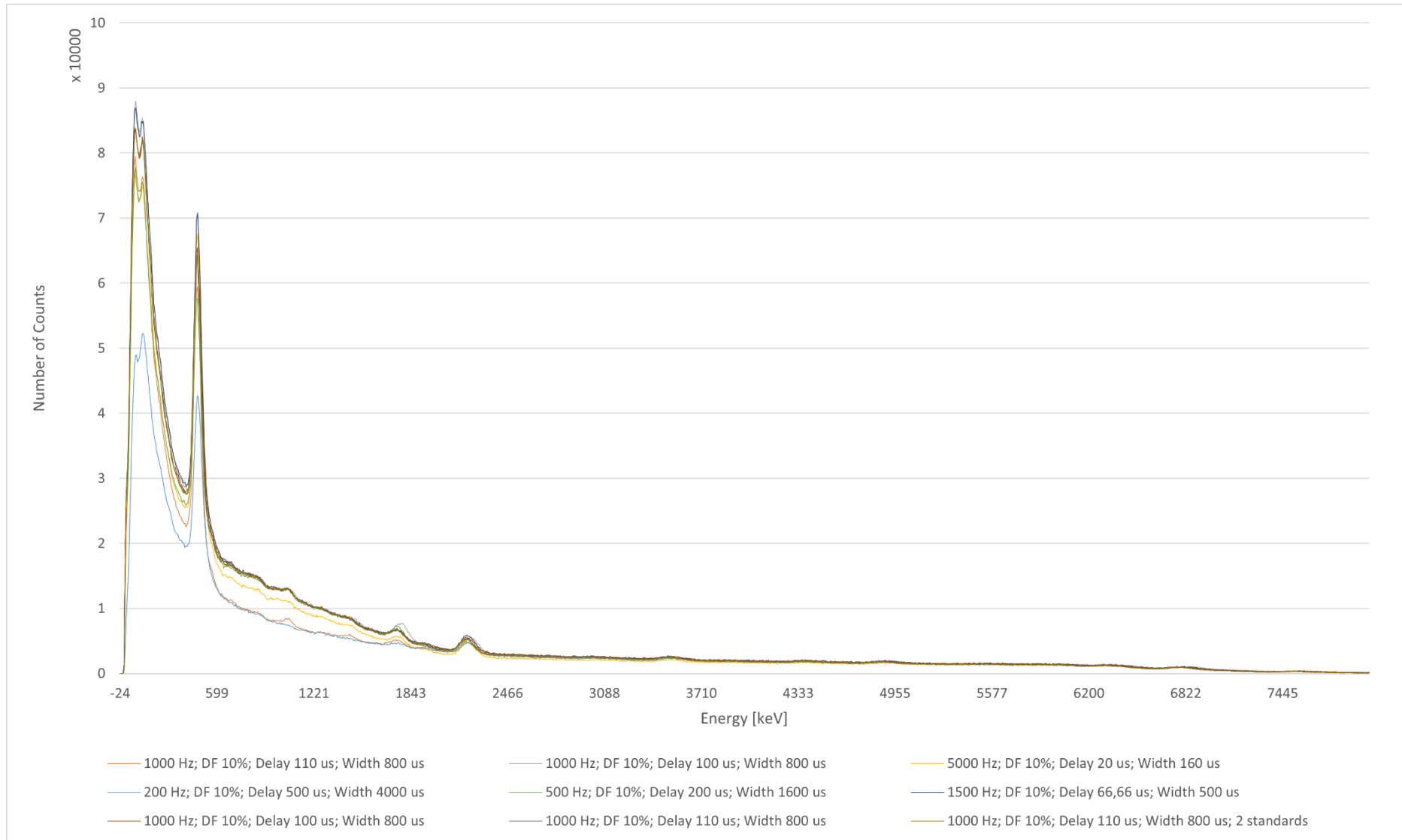
Figure 8.15: Measurements with different configurations of the NG.

Noticeable are dark orange and blue spectra, which actually did not contain any visible peaks in the higher energy range and therefore these configurations resulted in worse analysis than other spectra. A similar problem occurred when the beam current was set to 60 µA and voltage to 85 kV. The consequence of doing so was a 99.8% deadtime of the detector and acquisition of almost no usable data as seen in Figure 8.16. The reason for this effect was probably an enormous number of photons produced by the neutron activation and overload of the detector, which then lead to the photomultiplier tube "crashing" and not being able to continue in the measurement.
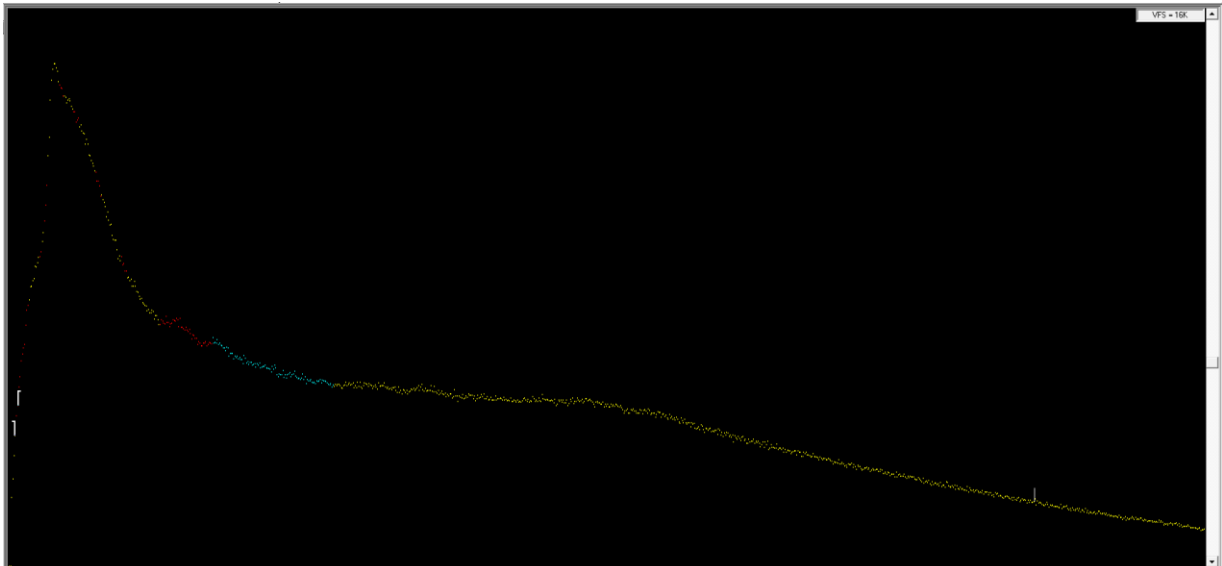
Figure 8.16: The overload of the spectrometer (beam current 60 µA, voltage 85 kV).

We met this issue once more when we were about to measure the gamma energy of activated hydrogen. Even though we were able to activate the hydrogen and form a distinct energy peak in the spectrum, the Compton continuum increased rapidly and we lost all other peaks in the lower energy range, due to the same mistake as in previous measurement – the overload of the detector caused by wrong configuration.

Figure 8.17: Activated hydrogen peak with overloaded Compton continuum (beam current 60 µA, voltage 85 kV).

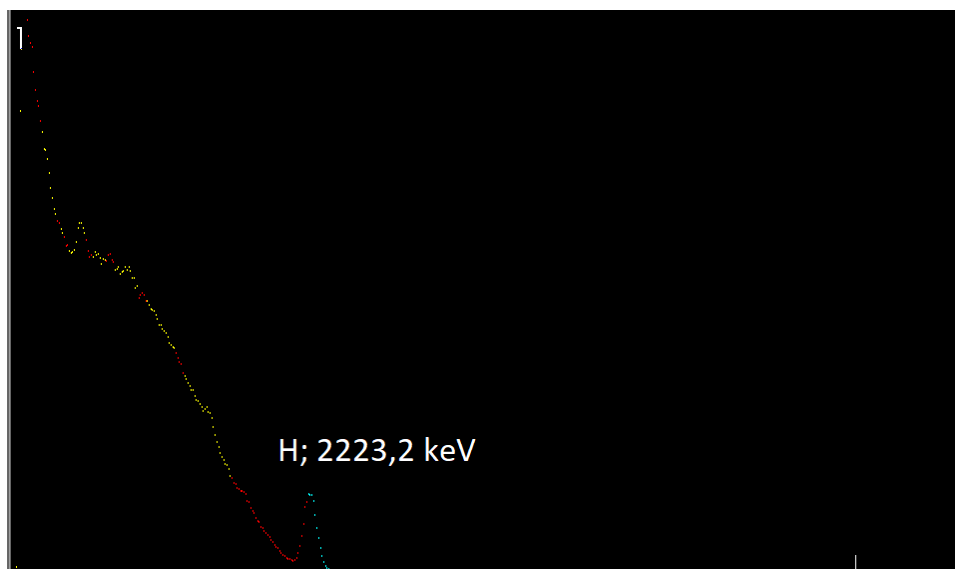### 8.4.4 Activated Nitrogen and Its 10,8 MeV Gamma-rays Energy

The energy level of 10,8 MeV of activated nitrogen was also in our interest as it is "the final energy level" in the higher energy range. The main objective was to find a peak at some channel that would correspond to this energy level, but luck was not on our side. I went through all of the measured spectra searching for at least a small hint of some peak appearing in the energy range between 10 MeV and 11 MeV, but every attempt has failed.

Two methods were used for searching for the peak. The first one is pretty simple – I went through every individual spectrum and I was zooming in on it trying to find a visible peak. If no peak was found, then I went through every data report of every single spectrum and searched through the actual number of counts at given channels near the 10,8 MeV value, but once more, there was no trace of the peak appearing, not even a slight increase in the number of counts.

The second method was a mathematical one – I tried to use the Gaussian process regression in order to locate inconspicuous peaks of small sizes, but I was met with the same problem as in the first method – there was no increase in the number of counts and therefore the mathematical method could not be used. Counts were still of the same numbers and order and if any channel collected a higher number of counts, it occurred only at one individual channel, therefore it could be interpreted as an error or a coincidence. The same process is used in the "Peak Analysis w/Report" algorithm within the Genie 2000 software. It was able to find peaks of Fe-54 that were not easily visible in the spectra, but as we could see in Table 8.10, the required nitrogen peak was not found.

After a thorough reading of the literature that focuses on the topic of 14 MeV activation of organic materials, and of the articles where similar experiments were described, I came to a conclusion of why we were not able to detect the 10,8 MeV energy of activated nitrogen. This peak usually appeared in spectra measured for hundreds of minutes, whereas our measurements lasted about 2 minutes on average. Also, the apparatus was usually sealed and absolutely shielded from the background radiation and other effects by using lead, so if they were to measure any increase in the 10 – 11 MeV energy range, they would only measure the 10,8 MeV nitrogen peak. Our laboratory is situated underground and effects of the surroundings, activation of the shielding and detector themselves and overall the imperfect environment prevented us from successful measurement of the nitrogen peak. In addition, the size of the standard used for the measurement also plays a role in the data acquisition as standards of small sizes emit less photons after their activation than those of larger sizes and thus peaks appearing in the spectrum are less distinct.

Conclusion

This thesis wraps around the calibration of high-volume gamma-ray spectrometer in a higher energy range. The theory part of the thesis went through the basics of nuclear physics and radiation detection, described the operation of neutron generators and explained the principles of gamma spectrometry. At the end of the theory part, the Neutron Activation Analysis was described as it plays the key role in the calibration, because thanks to the activation of certain elements, we were able to achieve energy levels above 3 MeV on which the calibration was performed.

In the practical part, the setup of used components and equipment was described and the configuration of the MP320 Neutron Generator was explained, because as we have learned, changes in the settings of the NG caused huge differences in gathered data and spectra. After that, 7 spectra were characterized from which the energy values and channels were used for the series of calibrations all adding up to the complete and final calibration.

Judging from verifications and measurement errors included in Table 8.11, the energy calibration can be considered effective. It is clear that the calibration will not always be perfect, mainly due to the problems mentioned in Section 8.4, but deviations in the higher energy range are small and will not drastically influence measurements in future. The successful energy calibration made the NaI(Tl) spectrometer suitable for identification of the peaks in the higher range and for many other uses in the future.

For future intentions one should pay attention to some of the issues that can occur:

- Inadequate choice of energy values for calibration
- Possible activation of Na within the NaI(Tl) crystal
- Incorrect NG configuration leads to a high dead-time
- Short time of measurement leads to less distinct peaks
- Choice of the software should be considered in advance

Lastly, we mentioned that the efficiency calibration is almost impossible to carry out due to the lack of information and inconsistency of the data acquisition. Although there are certain mathematical approaches to this matter, all of them lead to only estimates that we cannot rely on.

References

[1] P. A TIPLER,. and. A. LLEWELLYN. *Modern Physics*. 5th Edition. W. H. Freeman and Company, 2007. ISBN 978-0-7167-7550-8.

[2] ALEXA, Petr, Marie URBANOVÁ and Jaroslav HOFMANN. *Scriptum for the subject Physics II* at VŠB-TUO. [in Czech language]. Ústav fyziky a měřicí techniky VŠCHT Praha.

[3] KNOLL, Glenn F. Radiation Detection and Measurement /. 3rd ed. Michigan: John Wiley & Sons, 2000. ISBN 0-471-07338-5.

[4] Nucleus information resources. International Atomic Energy Agency, [cit. 2022-4-29]. Available at https://www.iaea.org/resources/nucleus-information-resources

[5] α, β, γ Penetration and Shielding. *Harvard Natural Sciences Lecture Demonstrations* [online]. [cit.2022-04-29].Available at: https://sciencedemonstrations.fas.harvard.edu/presentations/α-β-γ-penetration-and-shielding

[6] GILMORE, Gordon. *Practical Gamma-ray Spectrometry*. 2nd Edition. John Wiley & Sons, 2008. ISBN 978-0-470-86196-7.

[7] Beta particle. In: *Wikipedia: the free encyclopedia* [online]. San Francisco (CA): Wikimedia Foundation, 2001- [cit. 2022-04-29]. Available at: https://en.wikipedia.org/wiki/Beta_particle

[8] Gamma radiation. *ARPANSA: Australian Radiation Protection and Nuclear Safety Agency* [online]. [cit. 2022-04-29]. Available at: https://www.arpansa.gov.au/understanding-radiation/what-is-radiation/ionising-radiation/gamma-radiation X

[9] Ionizing Radiation: Background. *United States Department of Labor: Occupational Safety and Health Administration* [online]. [cit. 2022-04-29]. Available at: https://www.osha.gov/ionizing-radiation/background

[10] Decay chain. In: *Wikipedia: the free encyclopedia* [online]. San Francisco (CA): Wikimedia Foundation, 2001- [cit. 2022-04-29]. Available at: https://en.wikipedia.org/wiki/Decay_chain

[11] Uranium: The Uranium-238 Decay Chain. In: *United States Geological Survey: The Pubs Warehouse* [online]. [cit. 2022-04-29]. Available at: https://pubs.usgs.gov/of/2004/1050/uranium.htm

[12] Alpha particle. In: *Wikipedia: the free encyclopedia* [online]. San Francisco (CA): Wikimedia Foundation, 2001- [cit. 2022-04-29]. Available at: https://en.wikipedia.org/wiki/Alpha_particle

[13] VALKOVIĆ, Vladivoj. *14 MeV Neutrons: Physics and Applications* [online]. CRC Press, 2016 [cit. 2022-04-29]. ISBN 978-1-4822-3801-3.

[14] *Fundamental Physical Constants: The NIST reference on Constants, Units and Uncertainty* [online]. [cit. 2022-04-29]. Available at: https://physics.nist.gov/cuu/Constants/index.html

[15] WIRTZ, K. a K. H. BECKURTS. *Neutron Physics*. Berlin: Springer, 1964. ISBN 978-3-642-87616-5.

[16] NICO, Jeffrey a W. M. SNOW. Fundamental Neutron Physics. *Annual Review of Nuclear and Particle Science*. 2005(55). Available at: doi:10.1146/annurev.nucl.55.090704.151611

[17] MOLNÁR, Gábor. *Handbook of Prompt Gamma Activation Analysis with Neutron Beams*. Kluwer Academic Publishers, 2004. ISBN 978-1-4757-0997-1.

[18] BICHSEL, Hans. The Interaction of Radiation with Matter. *Detectors for Particles and Radiation.: Part 1: Principles and Methods* [online]. [cit. 2022-04-29]. ISBN 978-3-642-03606-4.

[19] Interaction of Radiation with Matter. *DOE Fundamentals Handbook: Nuclear Physics and Reactor Theory*. U.S. Department of Energy, 1993. DOE-HDBK-1019/1-93.

[20] NIKJOO, Hooshang, Shuzo UEHARA and Dimitris EMFIETZOGLOU. *Interaction of Radiation with Matter* [online]. CRC Press, 2012 [cit. 2022-04-29]. ISBN 978-1-4665-0960-3. Available at: https://books.google.com/books?id=5jnSBQAAQBAJ&pg=PA89&hl=cs&source=gbs_toc_r&cad=4#v=onepage&q&f=false

[21] Neutron Interaction with Matter. RINARD, P. *Passive Nondestructive Assay of Nuclear Materials*. U.S. Nuclear Regulatory Commission, NUREG/CR-5550, 1991. ISBN 0-16-032724-5.

[22] *National Nuclear Data Center: Evaluated Nuclear Data File* [online]. 2018 [cit. 2022-04-29]. Available at: https://www.nndc.bnl.gov/endf/

[23] *Radiation Protection and Safety of Radiation Sources: International Basic Safety Standards*. Vienna: International Atomic Energy Agency, 2011. ISBN 978–92–0–120910–8.

[24] *Practical Radiation Technical Manual: Personal Protective Equipment*. Vienna: International Atomic Energy Agency, 2004. IAEA-PRTM-5.

[25] LEROY, Claude a Pier-Giorgio RANCOITA. *Principles of Radiation Interaction with Matter and Detection*. 2nd Edition. Singapore: World Scientific Publishing Co. Pte., 2009. ISBN 978-981-281-827-0.

[26] O'KELLEY, G.D. *Detection and Measurement of Nuclear Radiation*. USA: Office of Technical Services, Department of Commerce. ISBN Detection and Measurement of Nuclear Radiation. NAS-NS 3105.

[27] TURNER, James E. *Atoms, Radiation, and Radiation Protection*. 3rd. Weinheim: Wiley-VCH, 2007. ISBN 978-3-527-40606-7.

[28] *Nucleide: Tables of evaluated data and comments on evaluation* [online]. [cit. 2022-04-29]. Available at: http://www.nucleide.org/DDEP_WG/DDEPdata.htm

[29] YANG, Jaemoon. *Deuterium: Discovery and Applications in Organic Chemistry*. Netherlands: Elsevier, 2016. ISBN 978-0-12-811040-9.

[30] *Tritium and Other Radionuclide Labeled Organic Compounds Incorporated in Genetic Materia*. National Council on Radiation Protection and Measurements, 1979. ISBN 0-91339247-2.

[31] VERMA, H.R. *Atomic and Nuclear Analytical Methods*. Berlin: Springer, 2007. ISBN 978-3-540-30277-3.

[32] GLASCOCK, Michael D. a Hector NEFF. Neutron activation analysis and provenance research in archaeology. *Measurement Science and Technology* [online]. IOP ebooks, 2003, 2003, (14/ Number 9) [cit. 2022-04-29]. Available at: https://iopscience.iop.org/article/10.1088/0957-0233/14/9/304

[33] PAHLAVANI, M.R., A. MOSTAAR a J. NADALI-VARKANI. Configuration of gamma detectors in a neutron interrogation system for detection of explosives. *Applied Radiation and Isotopes* [online]. 2018, (132) [cit. 2022-04-29]. ISSN 0969-8043. Available at: https://www.sciencedirect.com/science/article/pii/S0969804316307989

[34] Neutron-based methods for the detection of explosives. *Security Theory and Practice* [online]. Prague, 2017, **2017**(4) [cit. 2022-04-29]. ISSN 1801-8211. Dostupné z: https://veda.polac.cz/wp-content/uploads/2019/04/042017Neutron-based-methods-for-the-detection-of-explosives.pdf

[35] *5" x 3" x 16" scintillation detector for low background applications: Data Sheet*. Netherlands: Scionix Holland.

[36] MP320 Neutron Generator: Product Overview. *ThermoFisher Scientific* [online]. [cit. 2022-04-29]. Available at: https://www.thermofisher.com/order/catalog/product/1517021A

[37] GILMORE, Gordon. Appendix D: Gamma-Ray Energies in the Detector Background and the Environment. *Practical Gamma-ray Spectrometry*. 2nd Edition. John Wiley, 2008. ISBN 978-0-470-86196-7.

[38] VALKOVIĆ, Vladivoj. Irradiation of 4" x 4" NaI(Tl) detector by the 14 MeV neutrons. *Applied Radiation and Isotopes* [online]. Zagreb: Elsevier, 2010(68) [cit. 2022-04-29]. ISSN 0969-8043.